haematologica
Journal of the Ferrata Storti Foundation

Mmrn1 expression defines a novel subset of hematopoietic stem cells and leukemia stem cells with great self-renewal potential

by Naicheng Chen, Lijing Yang, Fang Chen, Hao Zeng, Xiaoyi Zhong, Yanying Liu, Zijin Chen, Mengying Yao, Yukai Lu, Mingqiang Shen, Mo Chen, Yang Xu, Song Wang, Xi Zhang, Junping Wang and Mengjia Hu

Received: February 18, 2025.
Accepted: January 9, 2026.

Citation: Naicheng Chen, Lijing Yang, Fang Chen, Hao Zeng, Xiaoyi Zhong, Yanying Liu, Zijin Chen, Mengying Yao, Yukai Lu, Mingqiang Shen, Mo Chen, Yang Xu, Song Wang, Xi Zhang, Junping Wang and Mengjia Hu. Mmrn1 expression defines a novel subset of hematopoietic stem cells and leukemia stem cells with great self-renewal potential.
Haematologica. 2026 Jan 22. doi: 10.3324/haematol.2025.287609 [Epub ahead of print]

Title page

Mmrn1 expression defines a novel subset of hematopoietic stem cells and leukemia stem cells with great self-renewal potential

Naicheng Chen[1,*], Lijing Yang[1,2,*], Fang Chen[1], Hao Zeng[1], Xiaoyi Zhong[3], Yanying Liu[1], Zijin Chen[3], Mengying Yao[3], Yukai Lu[1], Mingqiang Shen[1], Mo Chen[1], Yang Xu[1], Song Wang[1], Xi Zhang[4], Junping Wang[1,#], Mengjia Hu[1,5,#].

[1]State Key Laboratory of Trauma, Burns and Combined Injury, Institute of Combined Injury, Chongqing Engineering Research Center for Nanomedicine, College of Preventive Medicine, Third Military Medical University, Chongqing 400038, China.

[2]Medical Service Training Center, Chinese PLA General Hospital, Beijing, 100853, China.

[3]Department of Nephrology, the Key Laboratory for the Prevention and Treatment of Chronic Kidney Disease of Chongqing, Kidney Center of PLA, Xinqiao Hospital, Third Military Medical University, Chongqing, 400037, China.

[4]Medical Center of Hematology, Xinqiao Hospital, Third Military Medical University, Chongqing, 400037, China.

[5]Chinese PLA Center for Disease Control and Prevention, Beijing 100071, China.

*These authors contributed equally to this work.

[#]Correspondence:

Dr. Mengjia Hu. Email: humengjia3260@163.com or humengjia@tmmu.edu.cn.

Dr. & Prof. Junping Wang. Tel: +86-023-68771515; Fax: +86-023-68752009; Email: wangjunping@tmmu.edu.cn.

Running title: Mmrn1 defines a subset of HSCs and LSCs

Acknowledgements

We thank Prof. Jinyong Wang for gifting CD45.1 mice, Yang Liu for technical support in flow cytometry, and Xiaofan Lv for technical support in histopathological analysis.

Funding

This work was supported by grants from the National Key R&D Program of China (No. 2024YFA1107101), Natural Science Foundation of Chongqing City (No. CSTB2024NSCQ-JQX0002), National Natural Science Foundation of China (No. 82203974, 82430103), and Science Foundation of State Key Laboratory of Trauma and Chemical Poisoning (No. 2024K004).

Author contributions

N.C. and L.Y. designed the study, performed experiments, analyzed data and wrote the paper. F.C., H.Z. and X.Z. performed experiments and analyzed data. Y.L., Z.C., M.Y. and Y.L. participated in some animal experiments. M.S. and M.C. participated in data analysis. Y.X., S.W. and X.Z. participated in the initial experimental design and discussed the manuscript. M.H. and J.W. conceived and supervised the study, and revised the manuscript.

Disclosures

The authors declare no conflict of interest.

Data-sharing statement

The data and analyses conducted for this study are present in this article and supplementary material. Specifics of the bioinformatics analysis are detailed in the "Methods" section. The RNA-seq data of this article are available in the GEO database (No. GSE233828).

Abstract

Hematopoietic stem cells (HSCs) are critical for lifelong blood cell generation. After mutation accumulation and functional disruption, HSCs may transform into leukemic stem cells (LSCs), leading to malignant hematological disorders. However, both HSCs and LSCs are highly heterogeneous, which hinders our comprehensive understanding of their biological characteristics and clinical application. Here, we identified multimerin 1 (Mmrn1) as a reliable marker for the most primitive HSCs and LSCs. We found that Mmrn1 was abundantly present in human and mouse HSCs. Interestingly, HSCs with high levels of Mmrn1 displayed increased quiescence and regenerative capacity, accompanied by megakaryocytic lineage commitment. Importantly, Mmrn1 deficiency gradually impairs HSC self-renewal under stress of transplantation due to reduced quiescence. Additionally, we noticed that Mmrn1 was specifically upregulated in acute myeloid leukemia (AML) cells, and its overexpression predicted poor patient prognosis. Further investigation revealed that Mmrn1 marked a subset of quiescent LSCs responsible for AML initiation and development, and that deletion of Mmrn1 delays AML progression. Collectively, these data broaden our knowledge of stem cell heterogeneity in the context of normal and malignant hematopoiesis and advance the precision diagnosis and therapy of AML in the clinic.

Keywords: Mmrn1, hematopoietic stem cell, self-renewal, differentiation, acute myeloid leukemia

Introduction

Hematopoietic stem cells (HSCs) are a rare cell population that possesses the capacity to self-renew and differentiate into all lineages of blood cells throughout life.[1] The classical tree-like hierarchical model of hematopoiesis has been instrumental in understanding the step-by-step differentiation process of HSCs, but it raises confusing questions, such as the divergent states and functions of HSCs with similar immunophenotypes.[2,3] This heterogeneity poses a major challenge in elucidating the intrinsic properties and regulatory mechanisms.[4] Although recent single-cell RNA sequencing (scRNA-seq) technologies have provided insight into the characteristics of different HSC subpopulations, experimental evidence is still lacking.[5]

At present, a new model of hematopoietic differentiation, in which lineage determination occurs at the HSC level, has been proposed.[6,7] Some markers have been applied to discriminate distinct HSC subsets, but they are still often used in combination to improve identification accuracy.[8-10] In addition, HSCs can be transformed into leukemic stem cells (LSCs), also known as leukemia-initiating cells (LICs), when genetic and epigenetic mutations accumulate, therefore resulting in the development and progression of acute myeloid leukemia (AML).[11] Therefore, LSCs share many characteristics with HSCs, including cell cycle quiescence and strong self-renewal ability.[12,13] For instance, the presence of a dormant LSC subset is the root cause of AML chemoresistance and recurrence.[14] Therefore, identifying specific markers that can refine the analysis of HSCs and LSCs is urgent and of significant practical importance.

Multimerin 1 (Mmrn1), a member of the EMILIN protein family, is present in multiple tissues, including brain, muscle, skin and bone marrow (BM), as shown by the Human Protein Atlas database. Initially, Mmrn1 was reported to promote the

adhesion of platelets via binding to von Willebrand factor.[15] Additionally, Mmrn1 participates in modulating cell viability and thus affects tissue regeneration and repair.[15] Notably, Mmrn1 has been found to be overexpressed in a variety of cancers including cervical cancer and colorectal cancer, and its upregulation is positively correlated with poor patient prognosis.[16] In the hematopoietic system, Mmrn1 overexpression is also associated with the hemorrhagic symptoms of Quebec platelet disorder (QPD) and adverse outcomes in pediatric AML.[17,18] Although research has made some progress, the exact role of Mmrn1 in HSCs and LSCs remains to be fully elucidated.

In this study, we demonstrated that Mmrn1 was enriched predominantly in HSCs. However, HSCs did not express Mmrn1 uniformly, and those with high levels of Mmrn1 exhibited increased quiescence, regenerative capacity and megakaryocytic lineage commitment. Importantly, knockout of Mmrn1 reduced HSC quiescence, therefore impairing HSC self-renewal under stress of transplantation. Furthermore, Mmrn1 expression could identify LSCs with high leukemic initiation potential, and its deficiency inhibits AML progression. Collectively, our findings reveal that Mmrn1 is a reliable marker in distinguishing HSC heterogeneity and provide an effective observational indicator for the development and treatment of AML.

Methods

Animals

Wild-type (WT) C57BL/6J mice were purchased from Laipite Biotechnology Company (Chongqing, China). Mmrn1$^{+/eGFP}$ and NOD-Prkdc^{scid} Il2rg$^{em1/Smoc}$ (M-NSG) mice were obtained from the Model Organisms Center (Shanghai, China). Mmrn1$^{-/-}$ mice were purchased from Cyagen Biosciences Inc (Suzhou, China). Congenic CD45.1 mice were kindly gifted by Prof. Jinyong Wang. All the mice were male and

used at 6-8 weeks of age unless otherwise specified. All animal experiments were approved by the Animal Care Committee of Third Military Medical University (Chongqing, China).

Human samples

Human umbilical cord blood (UCB) samples were obtained from Southwest Hospital (The First Affiliated Hospital of Third Military Medical University), and then CD34+ cells were isolated using the Human CD34 Positive Selection kit (Stem Cell Technologies, Vancouver, Canada). BM specimens from AML patients and healthy volunteers were obtained from Daping Hospital (The Third Affiliated Hospital of Third Military Medical University). All participants provided informed consent, and the use of human UCB and BM samples were approved by the Institutional Review Board of Third Military Medical University (Chongqing, China).

Flow cytometry

Analysis of mouse or human hematopoietic cell phenotype, cell cycle, bromodeoxyuridine (BrdU) incorporation, apoptosis and ploidy distribution was carried out as we previously described.[19,20] Flow cytometry detection was conducted using a FACSVerse flow cytometer (BD Biosciences, San Jose, CA, USA), and data analysis was performed via FlowJo version 10.0 software (TreeStar, San Carlos, CA, USA). Cell sorting was performed on a FACSAria III sorter (BD Biosciences).

RNA sequencing (RNA-seq)

Total RNA was isolated from Mmrn1$^{-/low}$ and Mmrn1^{high} long-term HSCs (LT-HSCs). After quality assessment, samples were subjected to RNA-seq analysis at Sinotech Genomics Co., Ltd (Shanghai, China). Genes with a fold change > 2 and a P-value < 0.05 were considered differentially expressed genes (DEGs). The methods for

generating scatter plots and performing Gene Set Enrichment Analysis (GSEA) were described in our previous works.[21,22] All the data have been deposited in the Gene Expression Omnibus (GEO) database (No. GSE233828).

Statistical analysis

The experimental data were analyzed using the GraphPad Prism 10.1.2 software (La Jolla, CA, USA). The within-group variances were similar. Unpaired two-tailed Student's t-tests were used for two-group comparisons, and one-way analysis of variance (ANOVA) followed by Tukey's test was used for multiple-group comparisons. Kaplan-Meier survival curves were compared via the log-rank test. Correlation analysis was conducted by Spearman's correlation test. Each experiment was independently performed at least 3 times. The data are presented as the mean ± standard deviation (SD). *P < 0.05, **P < 0.01, and ***P < 0.001 are considered statistically significant.

Additional methods

Additional methods are provided in Supplementary Material. All antibodies and primers are listed in Supplementary Table S1 and Supplementary Table S2, respectively.

Results

Mmrn1 is highly expressed in primitive human and mouse HSCs.

Studies have shown that Mmrn1 is expressed in megakaryocytes/platelets and participates in regulating the process of blood clotting.[15,23] Interestingly, by analyzing the Atlas of Blood Cells database, we found that Mmrn1 is also enriched in human and mouse hematopoietic stem and progenitor cell (HSPC) populations (Figure 1A; Supplementary Figure S1A). Similar results were observed in the BloodSpot database (Supplementary Figure S1B). To confirm these findings, we purified various

hematopoietic cells from human UCB and mouse BM by flow cytometry (Supplementary Figure S1C, D). Subsequently, quantitative PCR (qPCR) analysis verified that Mmrn1 expression was higher in primitive HSCs than in other non-megakaryocytic hematopoietic cells (Figure 1B, C).

To further elucidate the characteristics of Mmrn1, we engineered a transgenic mouse model ($Mmrn1^{+/eGFP}$) by knocking eGFP into the Mmrn1 locus (Supplementary Figure S2A). The transgenic manipulation did not interfere with Mmrn1 expression or the hematopoietic homeostasis in the mice (Supplementary Figure S2B-E). Notably, we detected a small $eGFP^+$ population in the BM of $Mmrn1^{+/eGFP}$ mice, where Mmrn1 expression was observed in $eGFP^+$ but not $eGFP^-$ cells (Figure 1D, E). These data suggest that $Mmrn1^{+/eGFP}$ mice may be an ideal model for tracking Mmrn1 expression *in vivo*. Consistent with the above results, HSCs from these mice displayed relatively high mean fluorescence intensity (MFI) of eGFP (Supplementary Figure S2F). Alternatively, the majority of HSPCs, as well as megakaryocyte progenitors (MkPs), were significantly present within the $eGFP^+$ BM cells obtained from $Mmrn1^{+/eGFP}$ mice (Figure 1F). Therefore, Mmrn1 may be a reliable marker for distinguishing primitive HSCs.

Mmrn1 expression synchronizes with the HSC state after various stresses.

HSC behavior is closely related to the cell cycle state.[21,24] However, how to effectively identify the HSC state is also an issue that urgently needs to be addressed. Given that the expression of c-Kit is markedly disrupted following irradiation (IR) or 5-fluorouracil (5-FU) treatment, we utilized EPCR in conjunction with SLAM instead of conventional markers to define HSCs and therefore referred these cells as ESLAM-HSCs (Supplementary Figure S3A). Intriguingly, the expression of Mmrn1 tended to first decrease but then increase in ESLAM-HSCs, which was consistent with the

proportion of cells in G0 phase at the indicated time points (Figure 2A, B; Supplementary Figure S3B, C). Additionally, CD86 was used to replace Sca-1 as a reliable HSC marker under lipopolysaccharide (LPS) treatment condition, which can significantly affect Sca1 expression and result in its inability to stably label HSCs.[25] In the L86K-HSCs of the Mmrn1$^{+/eGFP}$ mice treated with LPS, the changes in Mmrn1 expression and G0 phase proportion were still strongly correlated (Supplementary Figure S3D-F). In particular, the expression of Mmrn1 increased with age, as HSCs tended to be more quiescent (Supplementary Figure S3G, H). Furthermore, *in vitro* culture experiments with the addition of known cell cycle regulatory factors also showed a clear negative correlation between Mmrn1 expression and HSC proliferation (Figure 2C-F). Hence, these results suggest that Mmrn1 expression may also be used to reflect the state of HSCs.

Mmrn1 expression distinguishes a distinct population of HSCs.

HSCs exhibit high heterogeneity and can be grouped into different subpopulations using various marking strategies.[3,26] Flow cytometry analysis of Mmrn1$^{+/eGFP}$ mice revealed that eGFP expression was variable in HSCs, which could be divided into Mmrn1$^{-/low}$ and Mmrn1^{high} groups (Figure 3A). A significant difference in Mmrn1 mRNA expression was detected between the two subsets (Figure 3B). Of note, we found that compared with Mmrn1$^{-/low}$ LT-HSCs, Mmrn1^{high} LT-HSCs had a higher percentage of cells in the G0 phase and incorporated less BrdU, suggesting that Mmrn1^{high} LT-HSCs are more quiescent (Figure 3C; Supplementary Figure S4A). However, the apoptosis rates did not significantly differ between these two groups (Supplementary Figure S4B). Similar phenomena were observed in HSCs marked by SLAM (Supplementary Figure S4C-E).

Next, Mmrn1$^{-/low}$ and Mmrn1^{high} LT-HSCs were isolated and subjected to RNA-seq analysis (Supplementary Figure S4F). The results showed that 505 genes were upregulated and 1253 genes were downregulated in Mmrn1^{high} LT-HSCs (Figure 3D). The GSEA results indicated that stemness and quiescence-associated signatures were enriched in Mmrn1^{high} LT-HSCs, whereas lineage differentiation, proliferation and mobilization-associated signatures were enriched in Mmrn1$^{-/low}$ LT-HSCs (Figure 3E). In line with these data, qPCR analysis also substantiated changes in genes involved in the cell cycle modulation (Supplementary Figure S4G). Overall, the data suggest that these two HSC populations may play different roles in the hematopoietic system.

Mmrn1^{high} HSCs exhibit robust hematopoietic regenerative capacity.

To further delineate the differences between Mmrn1$^{-/low}$ and Mmrn1^{high} LT-HSCs, we conducted additional assessments of these subsets. The *in vitro* assays show that Mmrn1^{high} LT-HSCs were capable of generating more daughter cells, accompanied by increased colony-forming ability (Figure 4A, B). Moreover, HSC transplantation (HSCT) experiments were performed to clarify the functional heterogeneity of LT-HSC subpopulations divided on the basis of Mmrn1 expression (Figure 4C). It was found that Mmrn1^{high} subpopulation-derived cells exhibited a gradually increasing percentage in the peripheral blood (PB) of recipient mice after the first and second HSCT (Figure 4D, E). Substantially different chimerism levels were also observed in the BM cell populations of the recipients, although lymphoid and myeloid lineage commitment were comparable between the two groups (Supplementary Figure S5A-E). It is known that the homing of HSCs to the BM microenvironment is a critical step for hematopoietic reconstitution after transplantation. However, the results indicated that the difference in transplantation outcomes did not originate from distinct homing abilities (Supplementary Figure S5F, G). Collectively, HSCs with high Mmrn1

expression may contribute more strongly to the maintenance of long-term hematopoiesis.

Mmrn1^{high} HSCs display megakaryocyte-biased differentiation.

Considering that Mmrn1 is also present in megakaryocytes/platelets, we speculated that HSCs with high Mmrn1 expression may be directed towards differentiating into megakaryocytic lineage. As anticipated, GSEA of the RNA-seq data indicated that genes associated with megakaryocyte development and differentiation programming were enriched in Mmrn1^{high} LT-HSCs (Figure 5A). Indeed, Mmrn1^{high} LT-HSCs expressed high levels of recognized megakaryocyte-related genes, accompanied by increased CD41^{+} frequency (Figure 5B, C). Consistently, treatment with TPO, a master cytokine that promotes megakaryopoiesis, induced Mmrn1 expression in the LT-HSCs of Mmrn1$^{+/eGFP}$ mice (Supplementary Figure S6A). Studies have shown that there is a shortcut of megakaryopoiesis during stress-induced hematopoiesis, in which megakaryocytes can be directly generated from HSCs without experiencing intermediate differentiation processes.[27-29] Therefore, the differentiation rate of the megakaryocytic lineage is significantly faster than that of other hematopoietic lineages in the early stages of hematopoietic reconstitution. In view of this finding, we then examined HSC-derived platelet production *in vivo* through short-term transplantation experiments. It was observed that Mmrn1^{high} LT-HSCs generated more premegakaryocyte/erythroid progenitors (PreMegEs) and MkPs in recipient mice (Figure 5D). Moreover, Mmrn1^{high} LT-HSCs had the potential to generate highly polyploid (≥ 8 N) megakaryocytes, which is in line with the *in vitro* culture results (Figure 5E, F). Of particular interest, analysis of the scRNA-seq data revealed that the expression of Mmrn1 was significantly upregulated in high-ploidy megakaryocytes, which are mainly responsible for producing platelets (Supplementary Figure S6B, C).

Expectedly, the platelet chimerism level was significantly increased in the PB of the recipients receiving Mmrn1^{high} LT-HSCs (Supplementary Figure S6D). These findings prove that Mmrn1 may be helpful for mapping the development and maturation of megakaryocytes.

Mmrn1 deficiency leads to the loss of HSC self-renewal potential.

To provide functional evidence, we generated Mmrn1 knockout (KO) mice (Supplementary Figure S7A, B). It was found that blood cell parameters were largely normal in Mmrn1-deficient mice at steady-state (Supplementary Figure S7C-G), which is consistent with a previous study.[23] Further analysis revealed that Mmrn1 deficiency only slightly but did not statistically significantly affect the phenotypes of HSPCs in the BM of mice (Figure 6A; Supplementary Figure S7H). Of note, we observed that the proportion of G0 phase cells was decreased in HSCs with Mmrn1 deficiency (Figure 6B). To assess whether Mmrn1 regulates HSC function, we performed a competitive transplantation assay (Figure 6C). Recipient mice transplanted with Mmrn1$^{-/-}$ BM cells displayed a gradual decrease in donor-derived chimerism levels in the PB (Figure 6D). Consistent with these data, limiting dilution assays revealed that the frequency of functional, although not phenotypic, HSCs was decreased in Mmrn1$^{-/-}$ mice (Figure 6E). The results were also obtained from human CD34^{+} cells with MMRN1 knockdown (Supplementary Figure S7I, J). These phenomena were similar to those from other HSC stemness regulators, such as Hlf, Ndn and Foxo3a.[30-32] Taken together, these data confirmed that Mmrn1 is involved in maintaining the self-renewal of HSCs under the stress of transplantation.

Mmrn1 is upregulated in AML, and its high expression predicts poor patient prognosis.

Previous studies reported that MMRN1 expression is correlated with the diagnosis, staging and prognosis of multiple cancers.[18,33] Interestingly, the analysis of public databases revealed that MMRN1 was remarkably upregulated in AML, whereas it was decreased in most cancers (Figure 7A). The results from other databases and our clinical samples validated the above findings (Supplementary Figure S8A, B). Meanwhile, high expression of MMRN1 was detected in different leukemia cell lines (Supplementary Figure S8C). On the basis of the French-American-British (FAB) classification, MMRN1 was found to be upregulated mainly in non-M3 AML (Supplementary Figure S8D). Further analysis of the AML dataset demonstrated that LSCs enriched for CD34 and/or CD38 expressed higher levels of MMRN1 (Supplementary Figure S8E). Similarly, the scRNA-seq data showed that MMRN1 was highly expressed in the malignant cells of AML specimens (Supplementary Figure S8F). A previous study reported that there two types of LSCs, lymphoid-primed multipotent progenitor (LMPP)-like LSCs and granulocyte-monocyte progenitor (GMP) LSCs, which exhibit distinct functional behaviors.[34] However, compared with GMP-like LSCs, MMRN1 expression was only slightly but not statistically significantly increased in LMPP-like LSCs (Supplementary Figure S8G).

We next analyzed the correlation between the expression of MMRN1 and the prognosis of AML patients. The receiver operating characteristic (ROC) curve clearly revealed that MMRN1 expression had good diagnostic performance in predicting AML prognosis (Figure 7B; Supplementary Figure S8H). In addition, we attempted to divide AML samples into $MMRN1^{low}$ and $MMRN1^{high}$ groups and found that MMRN1 expression was significantly associated with BM blasts, FAB classification, cytogenetics, cytogenetic risk and NPM1 mutation (Supplementary Table S3). Besides, AML patients with high MMRN1 expression presented a relatively poor risk

of relapse and a low overall survival rate (Figure 7C, D; Supplementary Figure S8I, J). In agreement with these findings, MMRN1^{high} AML cells were enriched with several pathways linked to leukemia development and progression, such as the PI3K-Akt signaling pathway and calcium signaling pathway (Figure 7E). To assess how MMRN1 is upregulated in AML, we performed transcription factor analysis using published chromatin immunoprecipitation-sequencing (ChIP-seq) data. It was observed that multiple hematopoietic transcription factors could bind to the promoter region of the MMRN1 gene, among which ERG had the highest correlation with MMRN1 in AML samples (Figure 7F; Supplementary Figure S9A, B). These results strongly suggest that MMRN1 can function as a biomarker in the diagnosis and prognosis of AML.

Mmrn1 high expression marks LSCs with increased quiescence and self-renewal. These findings prompted us to speculate that the high levels of Mmrn1 may be used to identify functional LSC subpopulations. We then constructed an MLL-AF9 leukemia model using Mmrn1$^{+/eGFP}$ mice and noted that Mmrn1 was differentially expressed in phenotypic LSCs (Figure 8A; Supplementary Figure S10A). Consistent with the above data, the LSC subset with high Mmrn1 expression was more quiescent than that with -/low Mmrn1 expression (Figure 8B). Serial replating assays revealed that Mmrn1^{high} cells formed more colonies in each replating (Figure 8C). Importantly, we found that the survival rate of recipients receiving Mmrn1^{high} LSCs was significantly declined (Figure 8D). In addition, the increases in mCherry^{+} cell percentage, white blood cell (WBC) count and Wright-Giemsa-stained leukemia cells indicated that Mmrn1^{high} LSCs caused more serious leukemia symptoms in the recipients (Figure 8E; Supplementary Figure S10B, C). Meantime, compared with those in recipients of Mmrn1$^{-/low}$ LSCs, more AML cell infiltration was found in the spleen, lung and liver

of recipients transplanted with Mmrn1^{high} LSCs (Supplementary Figure S10D, E). We also detected more progeny cells with leukemia initiation activity in the BM of recipients transplanted with Mmrn1^{high} LSCs, which was further verified by limiting dilution assays (Figure 8F; Supplementary Figure S10F). The above effects were more pronounced after re-transplantation (Supplementary Figure S10G-I). On the other hand, we isolated CD34^{+} cells from human AML cases with high or low expression of MMRN1 and performed a xenotransplantation assay. Likewise, MMRN1^{high} cells exhibited higher activity to initiate leukemia development in M-NSG mice (Supplementary Figure S11A, B). Particularly, the functional assays using Mmrn1-deficient mice provided substantial evidence that Mmrn1 contributed to AML progression (Supplementary Figure S11C-H).

Finally, to determine whether there is a direct link between Mmrn1 expression and megakaryocytic lineage involvement in AML, Mmrn1^{high} and Mmrn1$^{-/low}$ LSCs were isolated from mice and then cultured *in vitro* in the presence of TPO stimuli. It was observed that CD41 expression was comparable between the two groups after being cultured for 7 days (Supplementary Figure S11I), indicating that Mmrn1's megakaryocyte bias is only relevant to normal hematopoiesis not leukemogenesis. In summary, these findings indicate that Mmrn1^{high} LSCs have a greater advantage in promoting the development of leukemia.

Discussion

The rapid development of high-throughput sequencing and other innovative technologies has facilitated a deeper understanding of the stem cells within the hematopoietic system.[35] However, the heterogeneity of the immunophenotypically defined HSCs and LSCs hinders the progress of this research.[36,37] Thus, the precise identification of distinct stem cell subsets and an understanding of their unique

biological properties are crucial for advancing medical research and clinical diagnosis and therapy.[37] In this study, we demonstrated that Mmrn1 serves as a specific marker which not only enables the tracking of an HSC population with great self-renewal and megakaryocyte-biased differentiation potential but also reflects the severity and prognosis of AML.

Previous studies have indicated that Mmrn1 is a megakaryocyte/platelet lineage-specific gene.[38,39] In the present study, by analyzing different transcriptomic data, we found that Mmrn1 was also significantly enriched in human and mouse HSCs. The subsequent generation of the Mmrn1-eGFP reporter mouse model allowed us to track Mmrn1 expression easily *in vivo*. Under normal circumstances, most HSCs located in the BM microenvironment are in a dormant state.[40] When the BM is subjected to various stress injuries, resting HSCs can survive and then rapidly proliferate and differentiate to meet the body's need for blood cells.[41,42] Once hematopoietic reconstruction is complete, HSCs can return to the quiescent state via an ERK-dependent negative feedback mechanism.[43] Interestingly, our experimental results demonstrated that the dynamic alteration in Mmrn1 expression after irradiation, chemotherapy or LPS treatment was closely associated with the cell cycle state of HSCs. Therefore, these findings support the notion that Mmrn1 can function to determine the status of HSCs.

Over the years, the classical model of hematopoiesis has been gradually revised based on the identification of various biomarkers, such as CD41, Hdc, CD63 and Vwf, which distinguish different functional HSC subpopulations.[8,19,44,45] However, potential hematopoietic markers remain inadequately understood due to the rarity of some HSC subsets or limitations in detection technology.[35,46] In this work, we noticed that Mmrn1 was differentially expressed in phenotypic HSC populations and Mmrn1^{high}

HSCs presented increased quiescence and regenerative potential. These data imply that Mmrn1^{high} HSCs may play a more critical role in hematopoietic recovery under stress conditions. After that, using the Mmrn1 KO mice, we found that Mmrn1 is nearly dispensable for normal hematopoiesis at steady-state but is required to maintain HSC self-renewal under stress of transplantation. Mmrn1 has been identified as a secretory protein containing an EGF-like domain, which is unique among EMILIN family members.[16] This domain is involved in the regulation of various physiological processes, including cell growth, adhesion, and signal transduction.[47] By integrating these findings, we reasonably assume that HSCs may regulate themselves via the secretion of Mmrn1. Nevertheless, further experiments are needed to verify the mechanism that mediates the role of Mmrn1 in HSCs.

Furthermore, our research revealed a significant association between Mmrn1 expression and the megakaryocytic lineage commitment of HSCs. This relationship is supported by the enrichment of megakaryocytic development and differentiation programs in Mmrn1^{high} HSCs, as well as their increased capacity to generate platelets. These findings are consistent with those of a previous study showing that platelet-biased HSCs reside at the apex of the hematopoietic hierarchy.[45] It is well established that there are two different pathways for megakaryopoiesis, namely, the direct and stepwise differentiation pathways.[48] Intriguingly, a recent study elucidated that direct and stepwise differentiation routes produce niche-supporting and immune megakaryocytes, respectively, and that both types of megakaryocytes usually have lower ploidy.[27] In contrast, platelet-producing megakaryocytes have high ploidy, and are collectively produced via these two routes. Here, our experiments revealed that Mmrn1^{high} HSCs were more inclined to generate high-ploidy megakaryocytes, facilitating rapid platelet replenishment post-stress. However, Mmrn1 deficiency had

no effect on thrombopoiesis, hinting that Mmrn1 may be a non-functional marker for identifying HSCs biased toward platelet-producing megakaryocytes. Overall, these findings link the expression of Mmrn1 to the developmental program of HSCs.

In addition to normal hematopoiesis, leukemia, a malignant clonal disease in living organisms, has attracted our attention.[13] The sequencing data from multiple databases as well as our experimental results revealed that MMRN1 was specifically upregulated in AML cells and its expression is strongly correlated with the diagnosis and prognosis of AML, suggesting that MMRN1 can act as a new AML biomarker. There is a hypothesis that leukemia originates from LSCs, which share many similarities with HSCs but lack effective control of cell proliferation and differentiation.[37,49] Although there are still controversies, recent studies have provided evidence supporting LSC existence. Here, data from an MLL-AF9-derived AML mouse model emphasized that LSCs with high Mmrn1 expression presented enhanced activity to initiate leukemic development and its ablation suppressed leukemia progression, indicating that Mmrn1 may be a functional marker for a more aggressive subset of LSCs. Indeed, a previous study has shown that MMRN1 is one of the LSC17 signature,[50] which further consolidates our findings. Based on our current data, transient inhibition of Mmrn1 may pose a relatively low toxic risk to the normal hematopoiesis at steady-state. Therefore, targeted eradication of Mmrn1^{high} LSCs may be a promising strategy for treating AML. However, our study did not employ other AML mouse models, which may limit the widespread use of Mmrn1. Moreover, future research should focus on exploring the downstream effector molecules and pathways of Mmrn1 in AML.

In conclusion, we delineated the multifaceted role of Mmrn1 in hematopoiesis and its potential significance in AML. By revealing Mmrn1 as a marker for HSC status

and function, these findings lay a foundation for future research into the molecular basis of HSC heterogeneity. Furthermore, the prognostic relevance of Mmrn1 in AML also provides an opportunity for the development of new diagnostic tools and targeted therapeutic strategies.

References

1. Wilkinson AC, Igarashi KJ, Nakauchi H. Haematopoietic stem cell self-renewal in vivo and ex vivo. Nat Rev Genet. 2020;21(9):541-554.

2. Haas S, Trumpp A, Milsom MD. Causes and Consequences of Hematopoietic Stem Cell Heterogeneity. Cell Stem Cell. 2018;22(5):627-638.

3. Kucinski I, Campos J, Barile M, et al. A time- and single-cell-resolved model of murine bone marrow hematopoiesis. Cell Stem Cell. 2024;31(2):244-259.e10.

4. Eaves CJ. Hematopoietic stem cells: concepts, definitions, and the new reality. Blood. 2015;125(17):2605-2613.

5. Bandyopadhyay S, Duffy MP, Ahn KJ, et al. Mapping the cellular biogeography of human bone marrow niches using single-cell transcriptomics and proteomic imaging. Cell. 2024;187(12):3120-3140.e29.

6. Cheng H, Zheng Z, Cheng T. New paradigms on hematopoietic stem cell differentiation. Protein Cell. 2020;11(1):34-44.

7. Safina K, van Galen P. New frameworks for hematopoiesis derived from single-cell genomics. Blood. 2024;144(10):1039-1047.

8. Robin C, Ottersbach K, Boisset JC, Oziemlak A, Dzierzak E. CD41 is developmentally regulated and differentially expressed on mouse hematopoietic stem cells. Blood. 2011;117(19):5088-5091.

9. Lehnertz B, Chagraoui J, MacRae T, et al. HLF expression defines the human hematopoietic stem cell state. Blood. 2021;138(25):2642-2654.

10. Shin JY, Hu W, Naramura M, Park CY. High c-Kit expression identifies hematopoietic stem cells with impaired self-renewal and megakaryocytic bias. J Exp Med. 2014;211(2):217-231.

11. Yamashita M, Dellorusso PV, Olson OC, Passegue E. Dysregulated haematopoietic stem cell behaviour in myeloid leukaemogenesis. Nat Rev Cancer. 2020;20(7):365-382.

12. Lu Y, Yang L, Shen M, et al. Tespa1 facilitates hematopoietic and leukemic stem cell maintenance by restricting c-Myc degradation. Leukemia. 2023;37(5):1039-1047.

13. Weng H, Huang H, Wu H, et al. METTL14 Inhibits Hematopoietic Stem/Progenitor Differentiation and Promotes Leukemogenesis via mRNA m(6)A Modification. Cell Stem Cell. 2018;22(2):191-205.e9.

14. Dorrance AM, Neviani P, Ferenchak GJ, et al. Targeting leukemia stem cells in vivo with antagomiR-126 nanoparticles in acute myeloid leukemia. Leukemia. 2015;29(11):2143-53.

15. Jeimy SB, Tasneem S, Cramer EM, Hayward CP. Multimerin 1. Platelets. 2008;19(2):83-95.

16. Zhou Q, Liu Y, Zhou J, Zhang W. Prognostic value and immunological role of MMRN1: a rising star in cancer. Nucleosides Nucleotides Nucleic Acids. 2025;44(2):148-169.
17. Brunet JG, Sharma T, Tasneem S, et al. Thrombin generation abnormalities in Quebec platelet disorder. Int J Lab Hematol. 2020;42(6):801-809.
18. Laszlo GS, Alonzo TA, Gudgeon CJ, et al. Multimerin-1 (MMRN1) as Novel Adverse Marker in Pediatric Acute Myeloid Leukemia: A Report from the Children's Oncology Group. Clin Cancer Res. 2015;21(14):3187-3195.
19. Hu M, Lu Y, Wang S, et al. CD63 acts as a functional marker in maintaining hematopoietic stem cell quiescence through supporting TGFbeta signaling in mice. Cell Death Differ. 2022;29(1):178-191.
20. Chen S, Hu M, Shen M, et al. IGF-1 facilitates thrombopoiesis primarily through Akt activation. Blood. 2018;132(2):210-222.
21. Chen F, Lu Y, Xu Y, et al. Trim47 prevents hematopoietic stem cell exhaustion during stress by regulating MAVS-mediated innate immune pathway. Nat Commun. 2024;15(1):6787.
22. Hu M, Chen N, Chen M, et al. Transcription factor Nkx2-3 maintains the self-renewal of hematopoietic stem cells by regulating mitophagy. Leukemia. 2023;37(6):1361-1374.
23. Leatherdale A, Parker D, Tasneem S, et al. Multimerin 1 supports platelet function in vivo and binds to specific GPAGPOGPX motifs in fibrillar collagens that enhance platelet adhesion. J Thromb Haemost. 2021;19(2):547-561.
24. Shao L, Luo Y, Zhou D. Hematopoietic stem cell injury induced by ionizing radiation. Antioxid Redox Signal. 2014;20(9):1447-1462.
25. Kanayama M, Izumi Y, Yamauchi Y, et al. CD86-based analysis enables observation of bona fide hematopoietic responses. Blood. 2020;136(10):1144-1154.
26. Becker HJ, Ishida R, Wilkinson AC, et al. Controlling genetic heterogeneity in gene-edited hematopoietic stem cells by single-cell expansion. Cell Stem Cell. 2023;30(7):987-1000.e8.
27. Li JJ, Liu J, Li YE, et al. Differentiation route determines the functional outputs of adult megakaryopoiesis. Immunity. 2024;57(3):478-494.e6.
28. Carrelha J, Meng Y, Kettyle LM, et al. Hierarchically related lineage-restricted fates of multipotent haematopoietic stem cells. Nature. 2018;554(7690):106-111.
29. Yamamoto R, Morita Y, Ooehara J, et al. Clonal analysis unveils self-renewing lineage-restricted progenitors generated directly from hematopoietic stem cells. Cell. 2013;154(5):1112-1126.

30. Komorowska K, Doyle A, Wahlestedt M, et al. Hepatic Leukemia Factor Maintains Quiescence of Hematopoietic Stem Cells and Protects the Stem Cell Pool during Regeneration. Cell Rep. 2017;21(12):3514-3523.
31. Asai T, Liu Y, Di Giandomenico S, et al. Necdin, a p53 target gene, regulates the quiescence and response to genotoxic stress of hematopoietic stem/progenitor cells. Blood. 2012;120(8):1601-1612.
32. Miyamoto K, Araki KY, Naka K, et al. Foxo3a is essential for maintenance of the hematopoietic stem cell pool. Cell Stem Cell. 2007;1(1):101-112.
33. Wang Y, Zhou Z, Chen L, Li Y, Zhou Z, Chu X. Identification of key genes and biological pathways in lung adenocarcinoma via bioinformatics analysis. Mol Cell Biochem. 2021;476(2):931-939.
34. Goardon N, Marchi E, Atzberger A, et al. Coexistence of LMPP-like and GMP-like leukemia stem cells in acute myeloid leukemia. Cancer Cell. 2011;19(1):138-152.
35. Xie X, Liu M, Zhang Y, et al. Single-cell transcriptomic landscape of human blood cells. Natl Sci Rev. 2021;8(3):nwaa180.
36. Cao J, Yao QJ, Wu J, et al. Deciphering the metabolic heterogeneity of hematopoietic stem cells with single-cell resolution. Cell Metab. 2024;36(1):209-221.e6.
37. Boutzen H, Murison A, Oriecuia A, et al. Identification of leukemia stem cell subsets with distinct transcriptional, epigenetic and functional properties. Leukemia. 2024;38(10):2090-2101.
38. Adam F, Zheng S, Joshi N, et al. Analyses of cellular multimerin 1 receptors: in vitro evidence of binding mediated by alphaIIbbeta3 and alphavbeta3. Thromb Haemost. 2005;94(5):1004-1011.
39. Colombatti A, Spessotto P, Doliana R, Mongiat M, Bressan GM, Esposito G. The EMILIN/Multimerin family. Front Immunol. 2011;2:93.
40. Zhang Z, Lu Y, Qi Y, et al. CDK19 regulates the proliferation of hematopoietic stem cells and acute myeloid leukemia cells by suppressing p53-mediated transcription of p21. Leukemia. 2022;36(4):956-969.
41. Du C, Liu C, Yu K, et al. Mitochondrial serine catabolism safeguards maintenance of the hematopoietic stem cell pool in homeostasis and injury. Cell Stem Cell. 2024;31(10):1484-1500.e9.
42. Sudo T, Motomura Y, Okuzaki D, et al. Group 2 innate lymphoid cells support hematopoietic recovery under stress conditions. J Exp Med. 2021;218(5):e20200817.
43. Baumgartner C, Toifl S, Farlik M, et al. An ERK-Dependent Feedback Mechanism Prevents Hematopoietic Stem Cell Exhaustion. Cell Stem Cell. 2018;22(6):879-892.e6.

44. Chen X, Deng H, Churchill MJ, et al. Bone Marrow Myeloid Cells Regulate Myeloid-Biased Hematopoietic Stem Cells via a Histamine-Dependent Feedback Loop. Cell Stem Cell. 2017;21(6):747-760.e7.
45. Sanjuan-Pla A, Macaulay IC, Jensen CT, et al. Platelet-biased stem cells reside at the apex of the haematopoietic stem-cell hierarchy. Nature. 2013;502(7470):232-236.
46. Vanickova K, Milosevic M, Ribeiro Bas I, et al. Hematopoietic stem cells undergo a lymphoid to myeloid switch in early stages of emergency granulopoiesis. EMBO J. 2023;42(23):e113527.
47. Shi S, Ma T, Xi Y. A Pan-Cancer Study of Epidermal Growth Factor-Like Domains 6/7/8 as Therapeutic Targets in Cancer. Front Genet. 2020;11:598743.
48. Psaila B, Mead AJ. Single-cell approaches reveal novel cellular pathways for megakaryocyte and erythroid differentiation. Blood. 2019;133(13):1427-1435.
49. Fan R, Satilmis H, Vandewalle N, et al. Targeting S100A9 protein affects mTOR-ER stress signaling and increases venetoclax sensitivity in Acute Myeloid Leukemia. Blood Cancer J. 2023;13(1):188.
50. Ng SW, Mitchell A, Kennedy JA, et al. A 17-gene stemness score for rapid determination of risk in acute leukaemia. Nature. 2016;540(7633):433-437.

Figure Legends

Figure 1. Mmrn1 is highly expressed in primitive human and mouse HSCs. (A) scRNA-seq analysis of the expression of Mmrn1 in mouse BM cells (GSE128743) from the Atlas of Blood Cells database. (B) qPCR analysis of MMRN1 mRNA expression in the indicated hematopoietic cell populations purified from UCB cells (n = 3). The flow cytometric gating strategies are provided in Supplementary Figure S1C. Statistical differences were analyzed by comparing each group with HSCs. (C) qPCR analysis of Mmrn1 mRNA expression in the indicated hematopoietic cell populations purified from mouse BM (n = 3). The flow cytometric gating strategies are provided in Supplementary Figure S1D. Statistical differences were analyzed by comparing each group with LT-HSCs. (D) Representative flow cytometric plots showing the frequency of $eGFP^-$ and $eGFP^+$ BM cells from $Mmrn1^{+/+}$ and $Mmrn1^{+/eGFP}$ mice. (E) qPCR analysis of Mmrn1 mRNA expression in the sorted $eGFP^-$ or $eGFP^+$ BM cells from $Mmrn1^{+/eGFP}$ mice (n = 3). (F) The percentages of the indicated HSPC populations in total, $eGFP^-$ and $eGFP^+$ BM cells from $Mmrn1^{+/eGFP}$ mice (n = 6). HSPCs were distinguished by CD34 and Flk2 or SLAM family markers (CD150 and CD48), respectively. Representative flow cytometric plots are shown in the left. Data are shown as the mean ± SD. $^{**}P < 0.01$, $^{***}P < 0.001$.

Figure 2. Mmrn1 expression is synchronized with the HSC state after various stresses. (A) Flow cytometric analysis of Mmrn1-eGFP expression in ESLAM-HSCs from the BM of $Mmrn1^{+/eGFP}$ mice at the indicated time points after 5.0 Gy IR (n = 6

per time point). WT mice served as negative controls. Representative flow cytometric plots at 15 days after 5.0 Gy IR are shown in the left. MFI, mean fluorescence intensity. (B) Cell cycle analysis of ESLAM-HSCs from the BM of Mmrn1$^{+/eGFP}$ mice at the indicated time points after 5.0 Gy IR (n = 6 per time point). The flow cytometric gating strategies are provided in Supplementary Figure S3A. (C-F) LT-HSCs sorted from the BM of Mmrn1$^{+/eGFP}$ mice were cultured with polyinosinic:polycytidylic acid (pI:pC; 1 μg/mL), IL-6 (50 ng/mL), IL-3 (20 ng/mL), IFNβ1 (1000 units/mL) or Senexin B (5 μM), a CDK19 inhibitor, for 48 hours (n = 6). (C, E) Mmrn1-eGFP expression and (D, F) the percentage of BrdU^{+} cells in cultured LT-HSCs were analyzed by flow cytometry. Data are shown as the mean ± SD. ***P < 0.001.

Figure 3. Mmrn1 expression distinguishes a distinct population of HSCs. (A) The gating strategies for subsequent flow cytometric analysis and sorting of Mmrn1$^{-/low}$ and Mmrn1^{high} LT-HSCs from the BM of Mmrn1$^{+/eGFP}$ mice. (B) qPCR analysis of Mmrn1 mRNA expression in Mmrn1$^{-/low}$ and Mmrn1^{high} LT-HSCs sorted from the BM of Mmrn1$^{+/eGFP}$ mice (n = 3). (C) Cell cycle analysis of Mmrn1$^{-/low}$ and Mmrn1^{high} LT-HSCs from the BM of Mmrn1$^{+/eGFP}$ mice (n = 6). (D) The volcano plot showing DEGs between Mmrn1$^{-/low}$ and Mmrn1^{high} LT-HSCs. Representative DEGs are indicated in the plot. (E) GSEA of the RNA-seq data using HSC-related gene sets. Data are shown as the mean ± SD. ***P < 0.001.

Figure 4. Mmrn1^{high} HSCs exhibit robust hematopoietic regenerative capacity. (A) Mmrn1$^{-/low}$ and Mmrn1^{high} LT-HSCs were sorted from the BM of Mmrn1$^{+/eGFP}$ mice, and then cultured in SFEM medium (1×10^3 cells per well) for 10 days. The percentage of LSKs in culture was analyzed by flow cytometry (n = 4). (B) The single-cell clonal formation analysis of Mmrn1$^{-/low}$ and Mmrn1^{high} LT-HSCs in

methylcellulose medium (n = 4). (C-H) 5×10^2 Mmrn1$^{-/low}$ and Mmrn1^{high} LT-HSCs were mixed with 5×10^5 CD45.1 mouse BM cells and then transplanted into lethally irradiated CD45.1 mice. Sixteen weeks later, 1×10^6 BM cells from the first recipients were transplanted into lethally irradiated second CD45.1 recipients. (C) Schematic diagram of the first and second HSCT. (D, E) The percentage of donor-derived cells in the PB of recipients at the indicated time points after the (D) first and (E) second HSCT (n = 6). Representative flow cytometric plots at 16 weeks after the first and second HSCT are shown in the left, respectively. Data are shown as the mean ± SD. *P < 0.05, **P < 0.01, ***P < 0.001.

Figure 5. Mmrn1^{high} HSCs display megakaryocyte-biased differentiation. (A) GSEA of the RNA-seq data using megakaryocyte-related gene sets. (B) qPCR analysis of mRNA expression of the indicated genes in Mmrn1$^{-/low}$ and Mmrn1^{high} LT-HSCs sorted from the BM of Mmrn1$^{+/eGFP}$ mice (n = 3). (C) The percentage of CD41$^+$ cells in Mmrn1$^{-/low}$ and Mmrn1^{high} LT-HSCs from the BM of Mmrn1$^{+/eGFP}$ mice (n = 6). Representative flow cytometric plots are shown in the left. (D, E) 5×10^2 freshly sorted Mmrn1$^{-/low}$ and Mmrn1^{high} LT-HSCs were transplanted into lethally irradiated CD45.1 mice along with 5×10^5 CD45.1 mouse BM cells, and follow-up analysis was performed at 2 weeks after transplantation. (D) The percentages of the indicated hematopoietic progenitor cell populations from CD45.2$^+$ BM of the recipients (n = 6). Representative flow cytometric plots are shown in the left. (E) The ploidy distribution in CD41$^+$ cells from the CD45.2$^+$ BM of recipients (n = 6). Representative flow cytometric plots are shown in the left. (F) Representative images of Mmrn1$^{-/low}$ and Mmrn1^{high} LT-HSCs at 7 days after culture *in vitro*. Data are shown as the mean ± SD. **P < 0.01, ***P < 0.001.

Figure 6. Mmrn1 deficiency leads to the loss of HSC self-renewal potential. (A) The numbers of MPs, LSKs, LT-HSCs, ST-HSCs, MPPs and SLAM-HSCs in two tibias and femurs from WT and Mmrn1$^{-/-}$ mice (n = 6). Representative flow cytometric plots are shown in the left. (B) Cell cycle analysis of LT-HSCs from the BM of WT and Mmrn1$^{-/-}$ mice (n = 6). (C, D) 5×10^5 BM cells from the BM of WT and Mmrn1$^{-/-}$ mice were mixed with 5×10^5 CD45.1 mouse BM cells and then transplanted into lethally irradiated CD45.1 mice. Sixteen weeks later, 1×10^6 BM cells from the first recipients were transplanted into lethally irradiated second CD45.1 recipients. Then, the third round of transplantation was carried out in the same manner. (C) Schematic diagram of competitive BM transplantation. (D) The percentages of donor-derived cells in the PB of recipients at 16 weeks after the first, second and third HSCT were analyzed by flow cytometry (n = 6). Representative flow cytometric plots are shown in the left. (E) Limiting dilution analysis of the functional HSC frequency in the BM of WT and Mmrn1$^{-/-}$ mice (n = 10). Data are shown as the mean ± SD. *P < 0.05, **P < 0.01, ***P < 0.001.

Figure 7. Mmrn1 is upregulated in AML, and its high expression predicts poor patient prognosis. (A) The radar chart showing differential expression of MMRN1 between normal and tumor samples from the UCSC XENA database that integrates the data from TCGA (patients) and GTEx (healthy controls) database. (B) ROC analysis of the diagnostic performance of MMRN1 for the indicated binary classification from the UCSC XENA database. (C) The distribution of MMRN1 expression in the remission and relapse AML patients from the Vizome database, which is a visualization website of the BEAT-AML dataset. (D) Kaplan-Meier curves showing the survival rates of AML patients with low or high expression of MMRN1. The patient data were obtained from the TCGA database. (E) Kyoto Encyclopedia of

Genes and Genomes (KEGG) enrichment analysis showing upregulated pathways in MMRN1^{high} group (top 50%) compared with MMRN1^{low} group (bottom 50%) within AML samples from the TCGA database. (F) The correlation analysis of MMRN1 and ERG expression in AML samples from the TCGA database. Data are shown as the mean ± SD. ***P < 0.001.

Figure 8. Mmrn1 high expression marks LSCs with increased quiescence and self-renewal. (A-G) Lineage$^-$ (Lin$^-$) cells isolated from Mmrn1$^{+/eGFP}$ mice were transduced with MLL-AF9 retrovirus to generate pre-leukemic cells, which were then transplanted into 7.5 Gy irradiated WT mice. Twenty-five days after transplantation, Mmrn1$^{-/low}$ and Mmrn1^{high} LSCs were purified from the first recipients and were transplanted into 6.0 Gy irradiated second recipients. After another 25 days, LSCs purified from the second recipients were transplanted into the third WT recipients irradiated with 6.0 Gy. (A) The gating strategies for flow cytometric analysis or sorting of Mmrn1$^{-/low}$ and Mmrn1^{high} LSCs from the BM of the first recipients. (B) Cell cycle analysis of Mmrn1$^{-/low}$ and Mmrn1^{high} LSCs from the BM of the first recipients at 25 days after transplanted with pre-leukemic cells (n = 6). (C) Serial replating analysis of 500 Mmrn1$^{-/low}$ and Mmrn1^{high} LSCs sorted from the BM of the first recipients at 25 days after transplanted with pre-leukemic cells (n = 4). (D) Kaplan-Meier curves of the second recipients after transplanted with Mmrn1$^{-/low}$ and Mmrn1^{high} LSCs (n = 20). (E) The percentages of mCherry$^+$ cells in the PB and BM from the second recipients at 25 days after transplanted with Mmrn1$^{-/low}$ and Mmrn1^{high} LSCs (n = 6). Representative flow cytometric plots are shown in the left. (F) The percentages of c-Kit$^+$ mCherry$^+$ cells and LSCs in the BM of the second recipients at 25 days after transplanted with Mmrn1$^{-/low}$ and Mmrn1^{high} LSCs (n = 6). Representative flow cytometric plots are shown in the left. Data are shown as the

mean ± SD. ***P < 0.001.

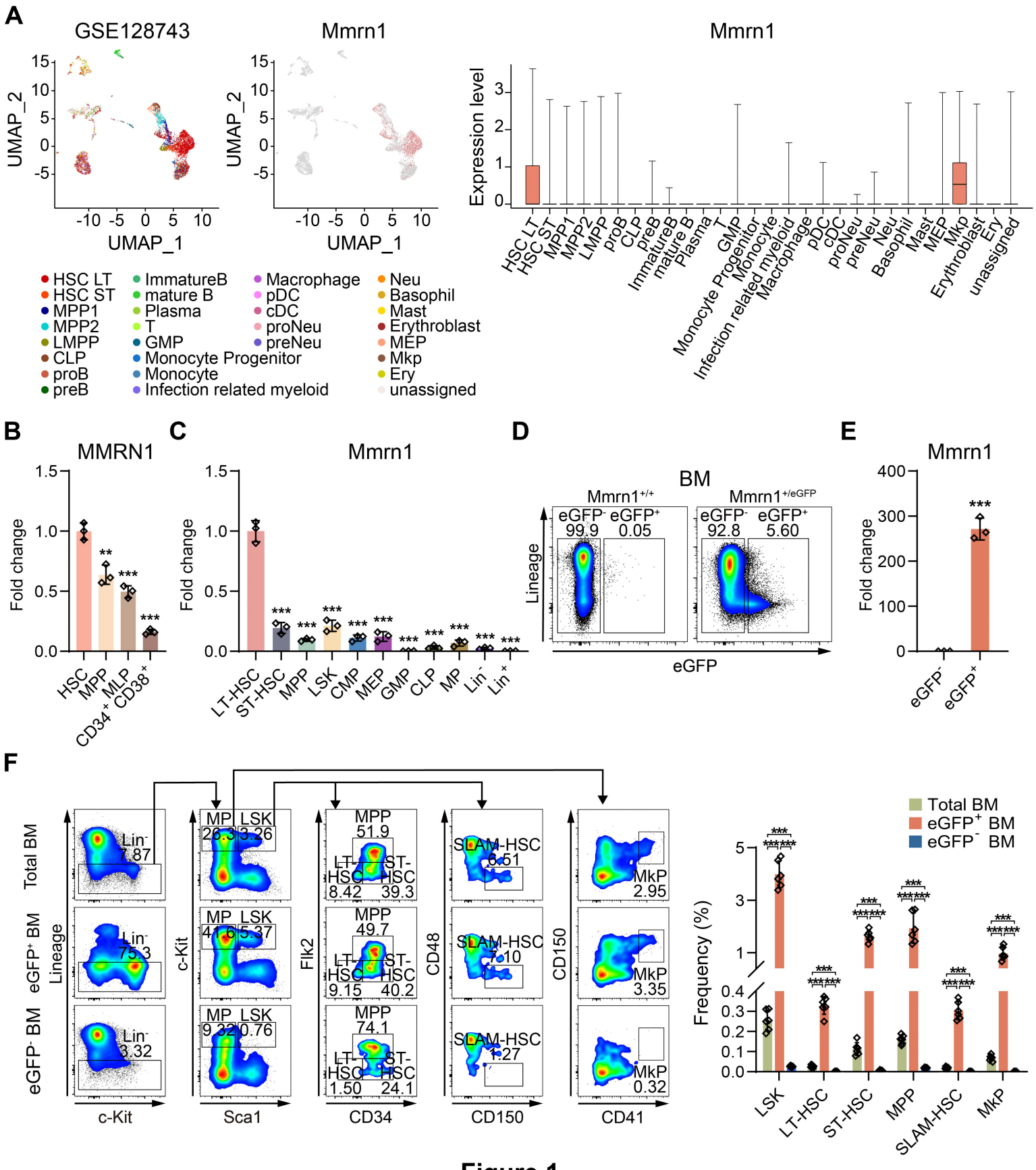
A
GSE128743
Mmrn1
Mmrn1
UMAP_2
UMAP_1
Expression level
HSC LT
HSC ST
MPP1
MPP2
LMPP
proB
CLP
preB
ImmatureB
mature B
Plasma
T
GMP
Monocyte Progenitor
Monocyte
Infection related myeloid
Macrophage
pDC
cDC
proNeu
preNeu
Neu
Basophil
Mast
MEP
Mkp
Erythroblast
Ery
unassigned
B
MMRN1
Fold change
HSC
MPP
MLP
CD34+ CD38+
C
Mmrn1
LT-HSC
ST-HSC
MPP
LSK
CMP
MEP
GMP
CLP
MP
Lin-
Lin+
D
BM
Mmrn1+/+
Mmrn1+/eGFP
eGFP- eGFP+
99.9 0.05
92.8 5.60
Lineage
eGFP
E
Mmrn1
Fold change
eGFP-
eGFP+
F
Total BM
eGFP+ BM
eGFP- BM
Lineage
c-Kit
Sca1
Flk2
CD34
CD48
CD150
CD41
Lin- 7.87
Lin- 75.3
Lin- 3.32
MP 26.3
LSK 3.26
MP 41.5
LSK 5.37
MP 9.32
LSK 0.76
MPP 51.9
LT-HSC 8.42
ST-HSC 39.3
MPP 49.7
LT-HSC 9.15
ST-HSC 40.2
MPP 74.1
LT-HSC 1.50
ST-HSC 24.1
SLAM-HSC 6.51
SLAM-HSC 7.10
SLAM-HSC 1.27
MkP 2.95
MkP 3.35
MkP 0.32
Total BM
eGFP+ BM
eGFP- BM
Frequency (%)
LSK
LT-HSC
ST-HSC
MPP
SLAM-HSC
MkP

Figure 1

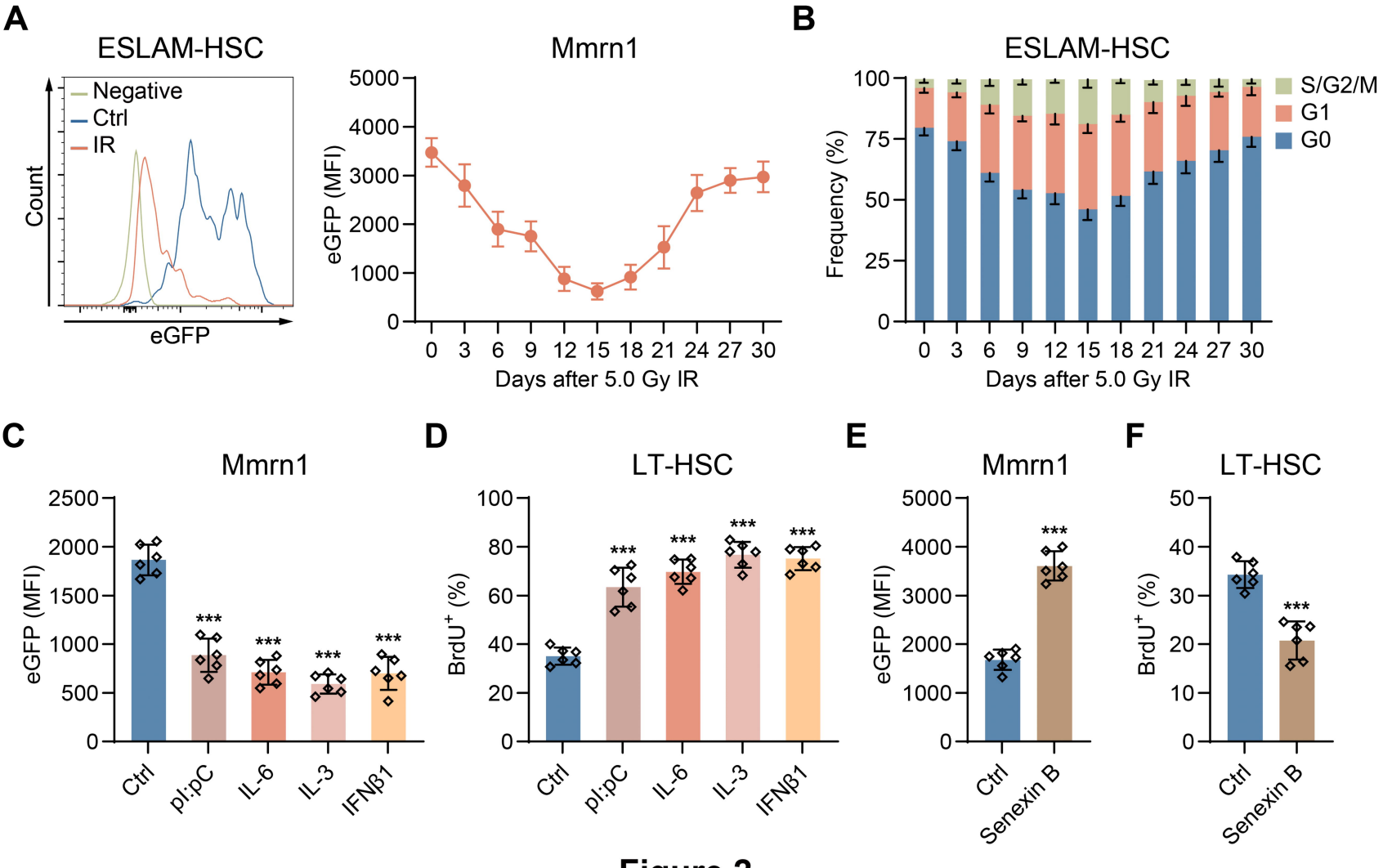
A
ESLAM-HSC
Negative
Ctrl
IR
Count
eGFP
Mmrn1
eGFP (MFI)
Days after 5.0 Gy IR
B
ESLAM-HSC
Frequency (%)
S/G2/M
G1
G0
Days after 5.0 Gy IR
C
Mmrn1
eGFP (MFI)
Ctrl
pI:pC
IL-6
IL-3
IFNβ1
D
LT-HSC
BrdU+ (%)
E
Mmrn1
eGFP (MFI)
Senexin B
F
LT-HSC
BrdU+ (%)

Figure 2

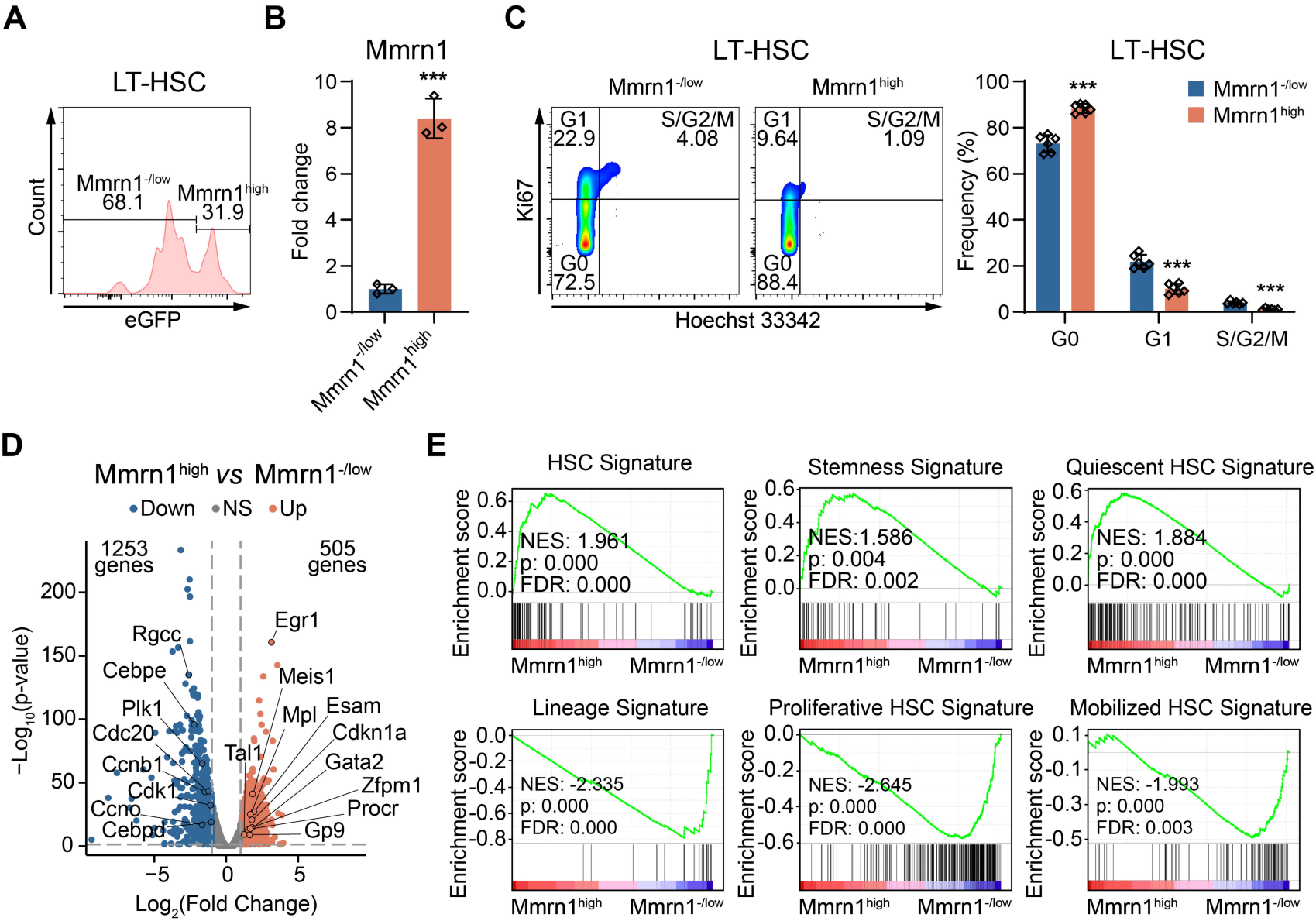
A
LT-HSC
Count
Mmrn1-/low
68.1
Mmrn1high
31.9
eGFP
B
Mmrn1
Fold change
***
Mmrn1-/low
Mmrn1high
C
LT-HSC
Mmrn1-/low
Mmrn1high
G1
22.9
S/G2/M
4.08
G0
72.5
G1
9.64
S/G2/M
1.09
G0
88.4
Ki67
Hoechst 33342
LT-HSC
Frequency (%)
Mmrn1-/low
Mmrn1high
***
G0
G1
S/G2/M
D
Mmrn1high vs Mmrn1-/low
Down
NS
Up
1253
genes
505
genes
−Log10(p-value)
Log2(Fold Change)
Rgcc
Cebpe
Plk1
Cdc20
Ccnb1
Cdk1
Ccno
Cebpd
Egr1
Meis1
Mpl
Esam
Cdkn1a
Tal1
Gata2
Zfpm1
Procr
Gp9
E
HSC Signature
NES: 1.961
p: 0.000
FDR: 0.000
Stemness Signature
NES:1.586
p: 0.004
FDR: 0.002
Quiescent HSC Signature
NES: 1.884
p: 0.000
FDR: 0.000
Lineage Signature
NES: -2.335
p: 0.000
FDR: 0.000
Proliferative HSC Signature
NES: -2.645
p: 0.000
FDR: 0.000
Mobilized HSC Signature
NES: -1.993
p: 0.000
FDR: 0.003
Enrichment score
Mmrn1high
Mmrn1-/low

Figure 3

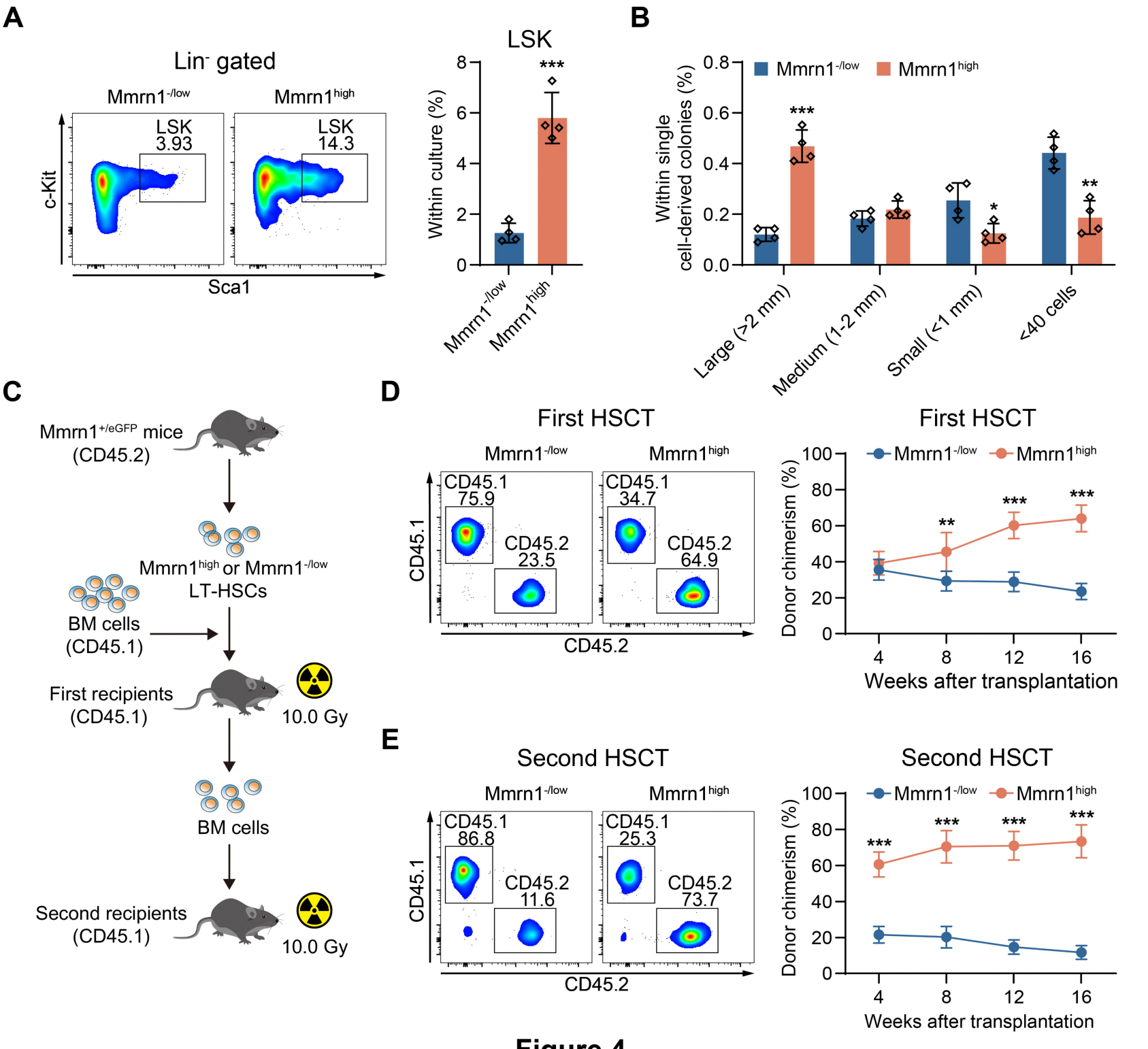
A
Lin- gated
Mmrn1-/low
Mmrn1high
LSK
3.93
LSK
14.3
c-Kit
Sca1
LSK
Within culture (%)
***
Mmrn1-/low
Mmrn1high
B
Mmrn1-/low
Mmrn1high
Within single cell-derived colonies (%)
***
*
**
Large (>2 mm)
Medium (1-2 mm)
Small (<1 mm)
<40 cells
C
Mmrn1+/eGFP mice
(CD45.2)
Mmrn1high or Mmrn1-/low
LT-HSCs
BM cells
(CD45.1)
First recipients
(CD45.1)
10.0 Gy
BM cells
Second recipients
(CD45.1)
10.0 Gy
D
First HSCT
Mmrn1-/low
Mmrn1high
CD45.1
75.9
CD45.2
23.5
CD45.1
34.7
CD45.2
64.9
CD45.1
CD45.2
First HSCT
Mmrn1-/low
Mmrn1high
Donor chimerism (%)
**
***
***
Weeks after transplantation
E
Second HSCT
Mmrn1-/low
Mmrn1high
CD45.1
86.8
CD45.2
11.6
CD45.1
25.3
CD45.2
73.7
CD45.1
CD45.2
Second HSCT
Mmrn1-/low
Mmrn1high
Donor chimerism (%)
***
***
***
***
Weeks after transplantation

Figure 4

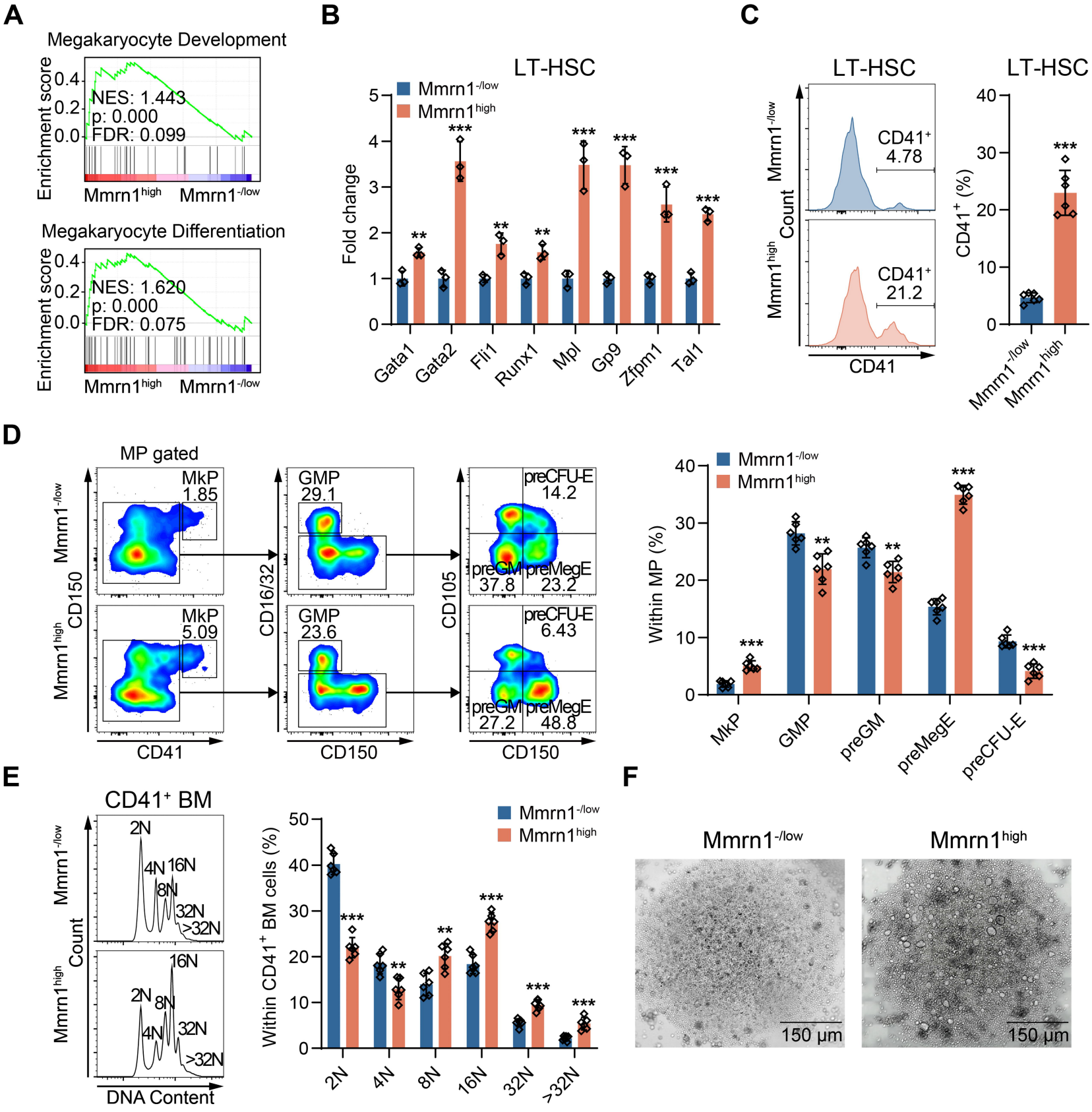
A
Megakaryocyte Development
Enrichment score
NES: 1.443
p: 0.000
FDR: 0.099
Mmrn1high
Mmrn1-/low
Megakaryocyte Differentiation
NES: 1.620
p: 0.000
FDR: 0.075
B
LT-HSC
Mmrn1-/low
Mmrn1high
Fold change
Gata1
Gata2
Fli1
Runx1
Mpl
Gp9
Zfpm1
Tal1
C
LT-HSC
CD41+ 4.78
CD41+ 21.2
Count
CD41
CD41+ (%)
D
MP gated
MkP 1.85
GMP 29.1
preCFU-E 14.2
preGM 37.8
preMegE 23.2
MkP 5.09
GMP 23.6
preCFU-E 6.43
preGM 27.2
preMegE 48.8
CD150
CD16/32
CD105
CD41
Within MP (%)
MkP
GMP
preGM
preMegE
preCFU-E
E
CD41+ BM
2N
4N
8N
16N
32N
>32N
DNA Content
Within CD41+ BM cells (%)
F
150 μm

Figure 5

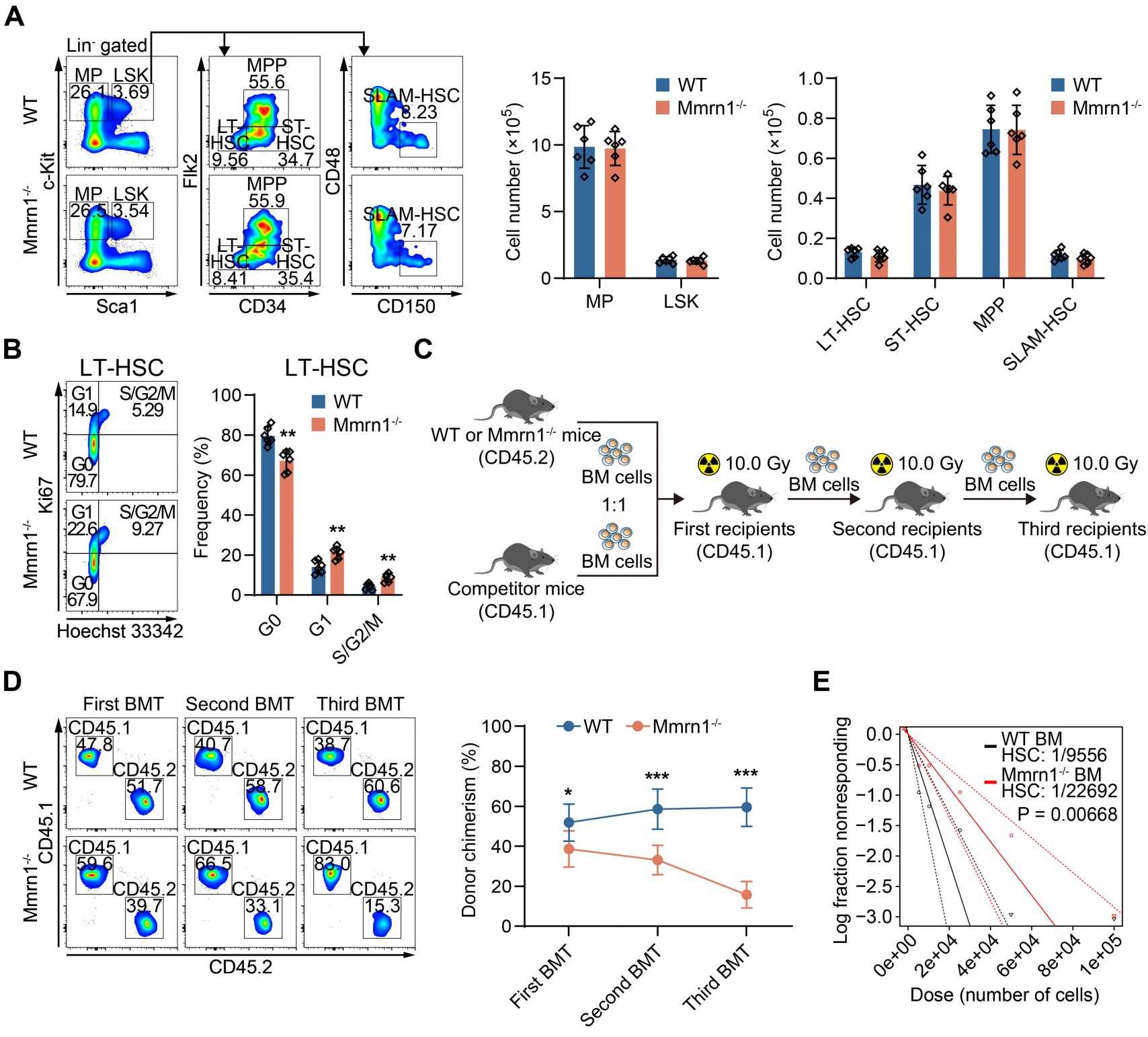
A
Lin- gated
WT
Mmrn1-/-
c-Kit
Sca1
MP
LSK
26.1
3.69
26.5
3.54
Flk2
CD34
MPP
55.6
55.9
LT-HSC
ST-HSC
9.56
34.7
8.41
35.4
CD48
CD150
SLAM-HSC
8.23
7.17
Cell number (×10^5)
WT
Mmrn1-/-
MP
LSK
LT-HSC
ST-HSC
MPP
SLAM-HSC
B
LT-HSC
G1
14.9
S/G2/M
5.29
G0
79.7
22.6
9.27
67.9
Ki67
Hoechst 33342
Frequency (%)
G0
G1
S/G2/M
C
WT or Mmrn1-/- mice
(CD45.2)
Competitor mice
(CD45.1)
BM cells
1:1
10.0 Gy
First recipients
(CD45.1)
Second recipients
(CD45.1)
Third recipients
(CD45.1)
D
First BMT
Second BMT
Third BMT
CD45.1
CD45.2
47.8
51.7
40.7
58.7
38.7
60.6
59.6
39.7
66.5
33.1
83.0
15.3
Donor chimerism (%)
E
Log fraction nonresponding
WT BM
HSC: 1/9556
Mmrn1-/- BM
HSC: 1/22692
P = 0.00668
Dose (number of cells)
0e+00
2e+04
4e+04
6e+04
8e+04
1e+05

Figure 6

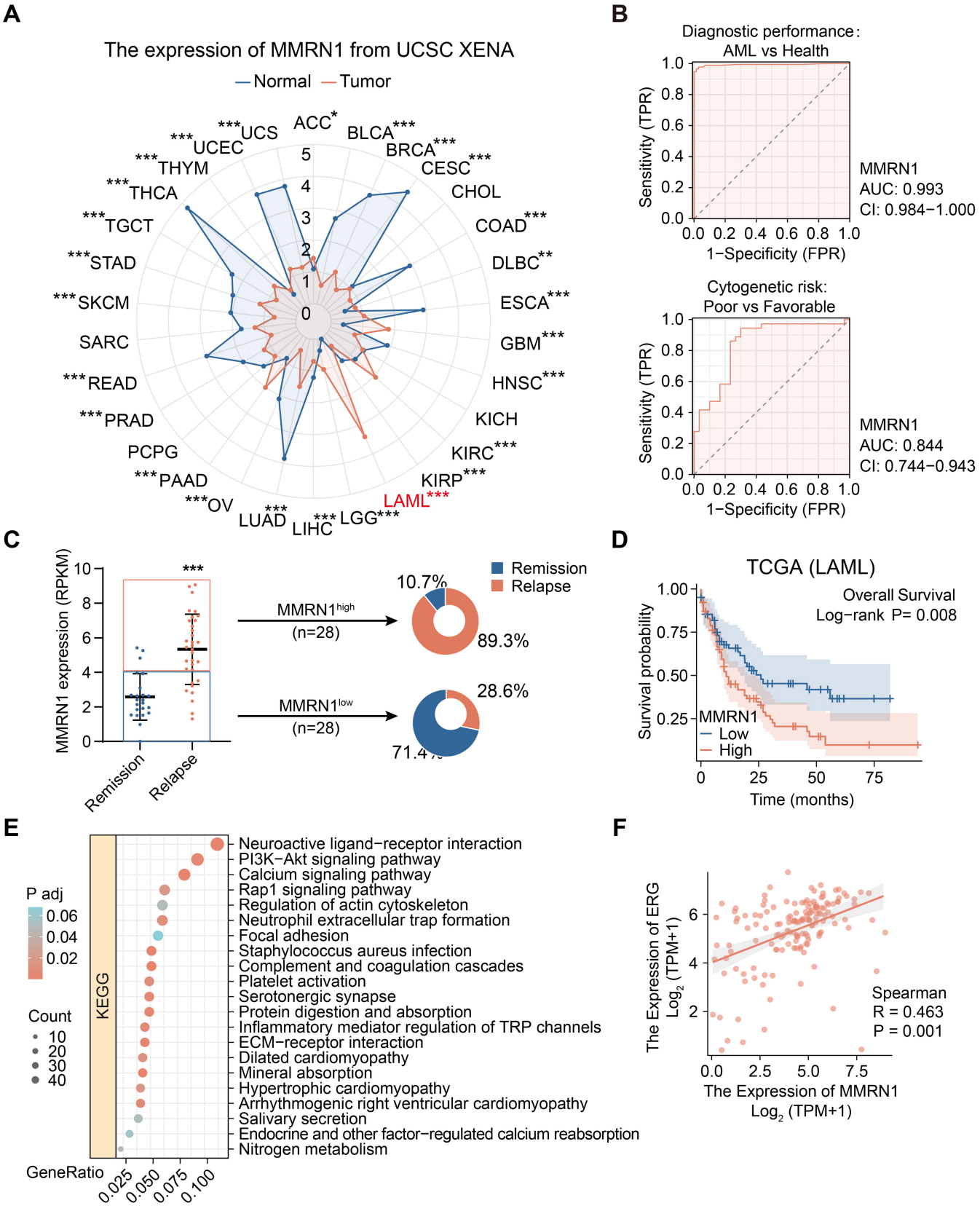
A
The expression of MMRN1 from UCSC XENA
Normal
Tumor
ACC*
BLCA***
BRCA***
CESC***
CHOL
COAD***
DLBC**
ESCA***
GBM***
HNSC***
KICH
KIRC***
KIRP***
LAML***
LGG***
LIHC***
LUAD***
OV***
PAAD***
PCPG
PRAD***
READ***
SARC
SKCM***
STAD***
TGCT***
THCA***
THYM***
UCEC***
UCS***
B
Diagnostic performance:
AML vs Health
Sensitivity (TPR)
1−Specificity (FPR)
MMRN1
AUC: 0.993
CI: 0.984−1.000
Cytogenetic risk:
Poor vs Favorable
MMRN1
AUC: 0.844
CI: 0.744−0.943
C
MMRN1 expression (RPKM)
Remission
Relapse
MMRN1high
(n=28)
MMRN1low
(n=28)
10.7%
89.3%
28.6%
71.4%
D
TCGA (LAML)
Overall Survival
Log−rank P= 0.008
Survival probability
MMRN1
Low
High
Time (months)
E
P adj
Count
KEGG
GeneRatio
Neuroactive ligand−receptor interaction
PI3K−Akt signaling pathway
Calcium signaling pathway
Rap1 signaling pathway
Regulation of actin cytoskeleton
Neutrophil extracellular trap formation
Focal adhesion
Staphylococcus aureus infection
Complement and coagulation cascades
Platelet activation
Serotonergic synapse
Protein digestion and absorption
Inflammatory mediator regulation of TRP channels
ECM−receptor interaction
Dilated cardiomyopathy
Mineral absorption
Hypertrophic cardiomyopathy
Arrhythmogenic right ventricular cardiomyopathy
Salivary secretion
Endocrine and other factor−regulated calcium reabsorption
Nitrogen metabolism
F
The Expression of ERG
Log2 (TPM+1)
The Expression of MMRN1
Log2 (TPM+1)
Spearman
R = 0.463
P = 0.001

Figure 7

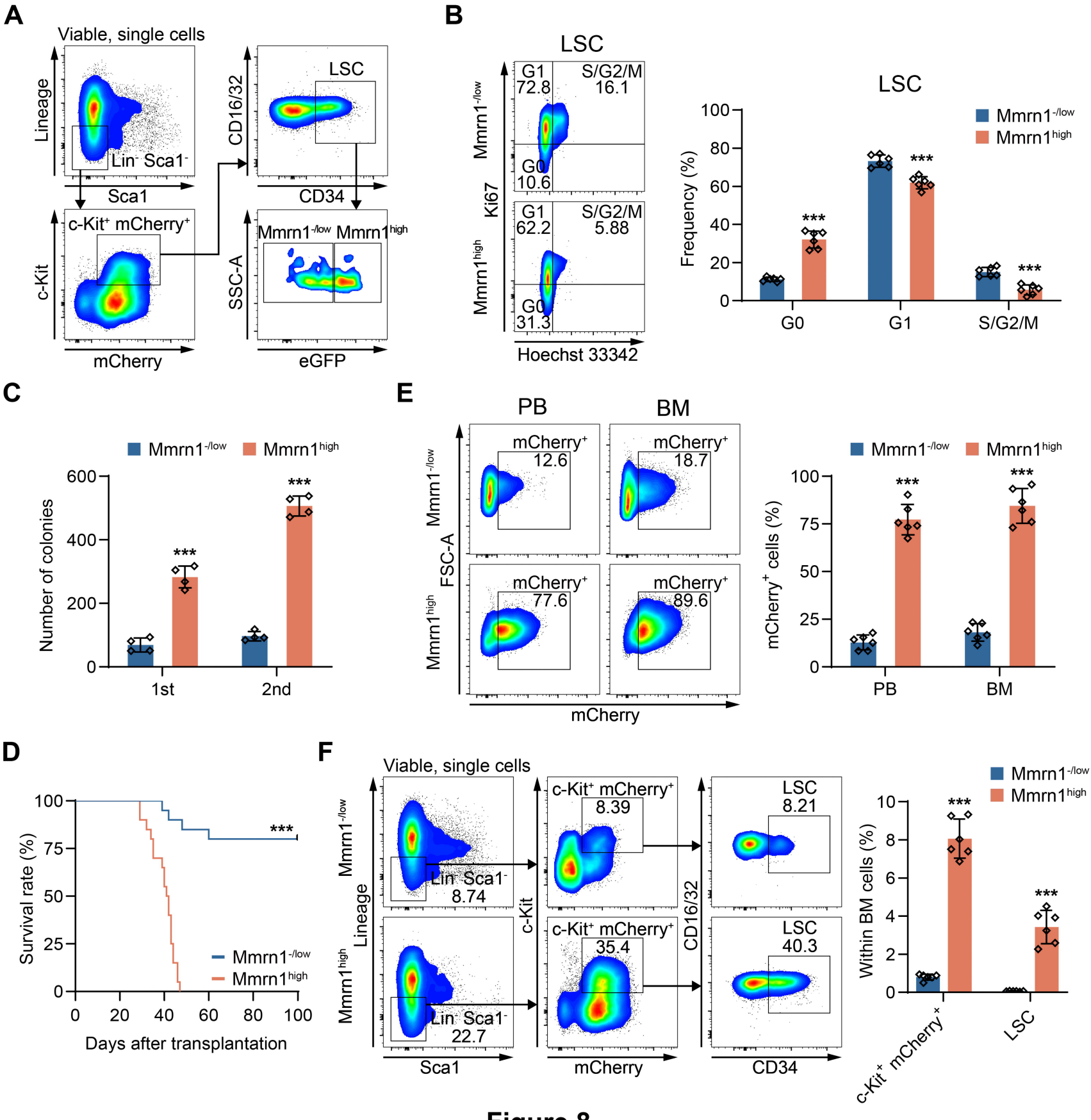
A
Viable, single cells
Lineage
Lin- Sca1-
Sca1
CD16/32
LSC
CD34
c-Kit+ mCherry+
c-Kit
mCherry
SSC-A
Mmrn1-/low Mmrn1high
eGFP
B
LSC
G1
72.8
S/G2/M
16.1
G0
10.6
G1
62.2
S/G2/M
5.88
G0
31.3
Mmrn1-/low
Ki67
Mmrn1high
Hoechst 33342
LSC
Mmrn1-/low
Mmrn1high
Frequency (%)
100
80
60
40
20
0
***
***
***
***
G0
G1
S/G2/M
C
Mmrn1-/low
Mmrn1high
Number of colonies
600
400
200
0
***
***
1st
2nd
E
PB
BM
mCherry+
12.6
mCherry+
18.7
mCherry+
77.6
mCherry+
89.6
Mmrn1-/low
Mmrn1high
FSC-A
mCherry
Mmrn1-/low
Mmrn1high
mCherry+ cells (%)
100
75
50
25
0
***
***
PB
BM
D
Survival rate (%)
100
75
50
25
0
***
Mmrn1-/low
Mmrn1high
0
20
40
60
80
100
Days after transplantation
F
Viable, single cells
Mmrn1-/low
Lineage
Lin- Sca1-
8.74
Mmrn1high
Lin- Sca1-
22.7
Sca1
c-Kit
c-Kit+ mCherry+
8.39
c-Kit+ mCherry+
35.4
mCherry
CD16/32
LSC
8.21
LSC
40.3
CD34
Mmrn1-/low
Mmrn1high
Within BM cells (%)
10
8
6
4
2
0
***
***
c-Kit+ mCherry+
LSC

Figure 8

Supplementary Material

Mmrn1 expression defines a novel subset of hematopoietic stem cells and leukemia stem cells with great self-renewal potential

Chen et al

Supplementary methods

HSC culture

For bulk HSC culture, 1×10^3 Mmrn1$^{-/low}$ and Mmrn1^{high} LT-HSCs were purified from the BM of Mmrn1$^{+/eGFP}$ mice and cultured in StemSpan SFEM medium (Stem Cell Technologies, Vancouver, Canada) containing 10 ng/ml SCF (PeproTech, Rocky Hill, NJ, USA), 20 ng/ml TPO (PeproTech), 10 μg/ml heparin (MedChemExpress, Monmouth Junction, NJ, USA) and 1% penicillin/streptomycin (Sigma, St. Louis, MO, USA). Ten days after culture, cells were collected for flow cytometric analysis. For single-cell colony formation assay, single Mmrn1$^{-/low}$ or Mmrn1^{high} LT-HSC was cultured with M3434 methylcellulose medium (Stem Cell Technologies) in U-bottom 96-well plates. Fourteen days after culture, colony size was analyzed under an inverted microscope.

Cell line culture

Human HS-5, HEL, HL-60, KG-1, NB-4, THP-1 and U-937 cells (Procell, Wuhan, China) were inoculated and cultured in RPMI-1640 medium (HyClone, South Logan, UT, USA) with 10% fetal bovine serum (HyClone).

qPCR analysis

This assay was carried out as we previously described.[1]

Lentiviral transfection

CD34$^+$ UCB cells were prestimulated for 12 hours in StemSpan SFEM medium (Stem Cell Technologies) with 100 ng/ml recombinant human SCF (PeproTech, Rocky Hill, NJ, USA), 100 ng/ml recombinant human Flt3L (PeproTech), 20 ng/ml recombinant human IL-6 (PeproTech), 20 ng/ml human recombinant TPO (PeproTech) and 1× penicillin/streptomycin (Beyotime Biotechnology, Shanghai, China). After that, the

transduction of lentivirus carrying shMMRN1 (labeled with mCherry) was performed in the same medium at a multiplicity of infection of 50-100 for 24 hours. Two to three days later, transduced cells were purified by flow cytometry based on mCherry expression and then used for further experiments. The core interference sequence of shRNA against MMRN1 is as follows: 5'-CTTGGACTATACCTGAGGAT-3'.

Stress treatment

For irradiation stress, Mmrn1$^{+/eGFP}$ mice were subjected to 5.0 Gy total body irradiation by a ^{60}Co irradiator (Third Military Medical University Irradiation Center,). For 5-FU treatment, Mmrn1$^{+/eGFP}$ mice were intraperitoneally injected with a single dose of 150 mg/kg 5-FU (Sigma). For LPS treatment, Mmrn1$^{+/eGFP}$ mice were intraperitoneally injected with a single dose of 5 mg/kg LPS (Beyotime Biotechnology, Shanghai, China). For *in vitro* stress, LT-HSCs from the BM of Mmrn1$^{+/eGFP}$ mice were cultured in SFEM medium with 1 μg/mL pI:pC (Sigma), 50 ng/mL IL-6 (PeproTech), 20 ng/mL IL-3 (PeproTech), 1000 units/mL IFNβ1 (R&D Systems, Minnesota, USA) or 5 μM SenexinB (MedChemExpress) for 48 h.

Transplantation assays

For HSCT assay, 5×10^2 freshly isolated Mmrn1$^{-/low}$ or Mmrn1^{high} LT-HSCs were mixed with 5×10^5 CD45.1 BM cells and then transplanted into lethally irradiated (10.0 Gy) CD45.1 mice. After 16 weeks, 1×10^6 BM cells from the first recipients were transplanted into the second recipients. At the indicated time points after the first and second HSCT, the chimerism levels in the recipients were detected by flow cytometry. For short-term transplantation assay, equal numbers of Mmrn1$^{-/low}$ or Mmrn1^{high} LT-HSCs (5×10^2) were transplanted into lethally irradiated CD45.1 mice, together with 5×10^5 CD45.1 BM cells. Two weeks post-transplantation, the PB and BM samples from recipients were analyzed by flow cytometry. For competitive

transplantation assay, 5×10^5 BM cells from WT or Mmrn1$^{-/-}$ mice, along with 5×10^5 CD45.1 BM cells, transplanted into lethally irradiated CD45.1 mice. After 16 weeks, 1×10^6 BM cells from the first recipients were transplanted into the second recipients. The third round of transplantation was carried out in the same manner. At the indicated time points after the first, second and third transplantation, the chimerism levels in the recipients were detected by flow cytometry.

Homing assay

This assay was performed as we previously described.[2,3] A total of 3×10^4 Mmrn1$^{-/low}$ and Mmrn1^{high} LT-HSCs freshly sorted from the BM of Mmrn1$^{+/eGFP}$ mice were labeled by 5,6-carboxyfluorescein diacetate succinimidyl ester (CFSE; Invitrogen, Carlsbad, CA, USA) and then transplanted into normal WT recipient mice irradiated with 10.0 Gy. After 16 h, CFSE$^+$ cell population in the BM of recipient mice was analyzed by flow cytometry. The homing efficiency was calculated as follows: homing efficiency = (CFSE$^+$ cell number in recipient BM/transplanted cell number)×100%.

Xenotransplantation assay

CD34$^+$ cells (2×10^5) isolated from the BM of AML patients with high or -/low expression of MMRN1 were transplanted into sublethally irradiated (2.5 Gy) M-NSG mice via intravenous injection. At 25 days after transplantation, the percentage of hCD45$^+$ cells in the PB of recipients were analyzed by flow cytometry. Meantime, the survival rates of mice were monitored.

Murine AML model establishment

For assessing the function of Mmrn1$^{-/low}$ and Mmrn1^{high} LSCs, retrovirus containing MSCV-MLL-AF9-IRES-mCherry vector was transduced into Lin$^-$ cells isolated from

the BM of Mmrn1$^{+/eGFP}$ mice. Next, pre-leukemic cells (mCherry^{+}) were sorted from the transduced cells and were transplanted into 7.5 Gy-irradiated WT mice. Twenty-five days after transplantation, 2×10^3 Mmrn1$^{-/low}$ and Mmrn1^{high} LSCs were purified from the first recipients and transplanted into the second WT recipients irradiated with 6.0 Gy. After another 25 days, 2×10^3 LSCs purified from the second recipients were transplanted into the third WT recipients irradiated with 6.0 Gy. For assessing the function of WT and Mmrn1$^{-/-}$ LSCs, MLL-AF9-induced leukemia model was established as mentioned above. After that, pre-leukemic cells (mCherry^{+}) were transplanted into 7.5 Gy-irradiated WT mice. Twenty-five days after transplantation, 2×10^3 LSCs purified from the first recipients and transplanted into the second WT recipients irradiated with 6.0 Gy.

Serial replating assay

Freshly sorted LSCs (5×10^2) were seeded in MethoCultTM M3434 medium (Stem Cell Technologies). After 7 days of culture, colonies were counted and then harvested for replating.

Limiting dilution assays

For assessing the functional HSC frequency, BM cells (5×10^3, 1×10^4, 2.5×10^4, 5×10^4 or 1×10^5) obtained from WT or Mmrn1$^{-/-}$ mice, along with CD45.1 BM cells (5×10^5), were transplanted into lethally irradiated CD45.1 recipient mice. In addition, CD34^{+} cells (1×10^4, 2.5×10^4, 5×10^4 or 1×10^5) transfected with shCtrl or shMMRN1 were transplanted into sublethally irradiated M-NSG mice. For assessing the functional LSC frequency, mCherry^{+} BM cells (5×10^2, 2.5×10^3, 5×10^3 or 1×10^4) were obtained from the first recipients reconstructed with Mmrn1$^{-/low}$ and Mmrn1^{high} LSCs. Then, these cells were transplanted into sublethally irradiated WT recipient mice. The frequency of functional HSCs or LSCs were analyzed as we previously reported.[4]

PB counts

PB samples were collected from the tail vein of leukemia mice and diluted in a 1% EDTA solution. White blood cell (WBC), red blood cell (RBC) and platelet (PLT) counts were measured by the Sysmex XT2000i hematology analyzer (Sysmex, Kobe, Japan).

Megakaryocytic differentiation induction

Freshly sorted Mmrn1^{high} and Mmrn1$^{-/low}$ LSCs were cultured in vitro in the presence of TPO stimulation, according to our previous protocol.[5] After 7 days of culture, CD41 expression was analyzed by flow cytometry.

Histology analysis

PB smears were fixed with methanol and stained with Wright-Giemsa (Beyotime Biotechnology) according to the manufacturer's protocol. Mouse spleen, lung and liver were fixed in zinc formalin (Solarbio, Shanghai, China) for 48 hours and then dehydrated in ethanol, embedded in paraffin, sectioned and stained with hematoxylin and eosin (Beyotime Biotechnology). These samples were scanned on a KF-PRO-020 Digital Pathology Slide Scanner (KFBIO, Ningbo, China).

Public database analysis.

The bulk RNA-seq data for Mmrn1 expression analysis in human and mouse hematopoietic cells were obtained from the BloodSpot database (https://www.bloodspot.eu/). The scRNA-seq data for Mmrn1 expression analysis in human and mouse hematopoietic cells were obtained from the Atlas of blood cells database (http://abc.sklehabc.com/) under reference number GSE150774, GSE128743 and GSE139369. The data on Mmrn1 expression in mouse megakaryocytes were derived from the OMIX database (https://ngdc.cncb.ac.cn/omix/) under reference

number OMIX005321. The AML clinical data were obtained from the UCSC XENA database (https://xena.ucsc.edu/), UALCAN database (https://ualcan.path.uab.edu/) and Vizome database (http://www.vizome.org/). The data applied to survival curve analysis of AML patients were downloaded from the TCGA database (https://tcga-data.nci.nih.gov/tcga/), PrognoScan database (http://dna00.bio.kyutech.ac.jp/PrognoScan/) and Kaplan-Meier plotter database (https://kmplot.com/analysis/). The data used for KEGG enrichment analysis were obtained from the TCGA database, and the data used for transcription factor binding analysis were obtained from the BloodChIP Xtra database (https://bloodchipxtra.vafaeelab.com/). For analyzing the expression of MMRN1 in GMP-like LSCs and LMPP-like LSCs, the data derived from a previous study was employed.[6] The R packages include pROC (v1.18.0), ggplot2 (v3.3.6), survival (v3.3.1), survminer (v0.4.9), DESeq2 (v1.36.0), edgeR (v3.38.2) and clusterProfiler (v4.4.4).

References

1. Lu Y, Zhang Z, Wang S, et al. Srebf1c preserves hematopoietic stem cell function and survival as a switch of mitochondrial metabolism. Stem Cell Reports. 2022;17(3):599-615.

2. Chen N, Quan Y, Chen M, et al. Melanocortin/MC5R axis regulates the proliferation of hematopoietic stem cells in mice after ionizing radiation injury. Blood Adv. 2023;7(13):3199-3212.

3. Hu M, Zeng H, Chen S, et al. SRC-3 is involved in maintaining hematopoietic stem cell quiescence by regulation of mitochondrial metabolism in mice. Blood. 2018;132(9):911-923.

4. Chen F, Lu Y, Xu Y, et al. Trim47 prevents hematopoietic stem cell exhaustion during stress by regulating MAVS-mediated innate immune pathway. Nat Commun. 2024;15(1):6787.

5. Chen S, Hu M, Shen M, et al. IGF-1 facilitates thrombopoiesis primarily through Akt activation. Blood. 2018;132(2):210-222.

6. Goardon N, Marchi E, Atzberger A, et al. Coexistence of LMPP-like and GMP-like leukemia stem cells in acute myeloid leukemia. Cancer Cell. 2011;19(1):138-52.

Supplementary Figure S1

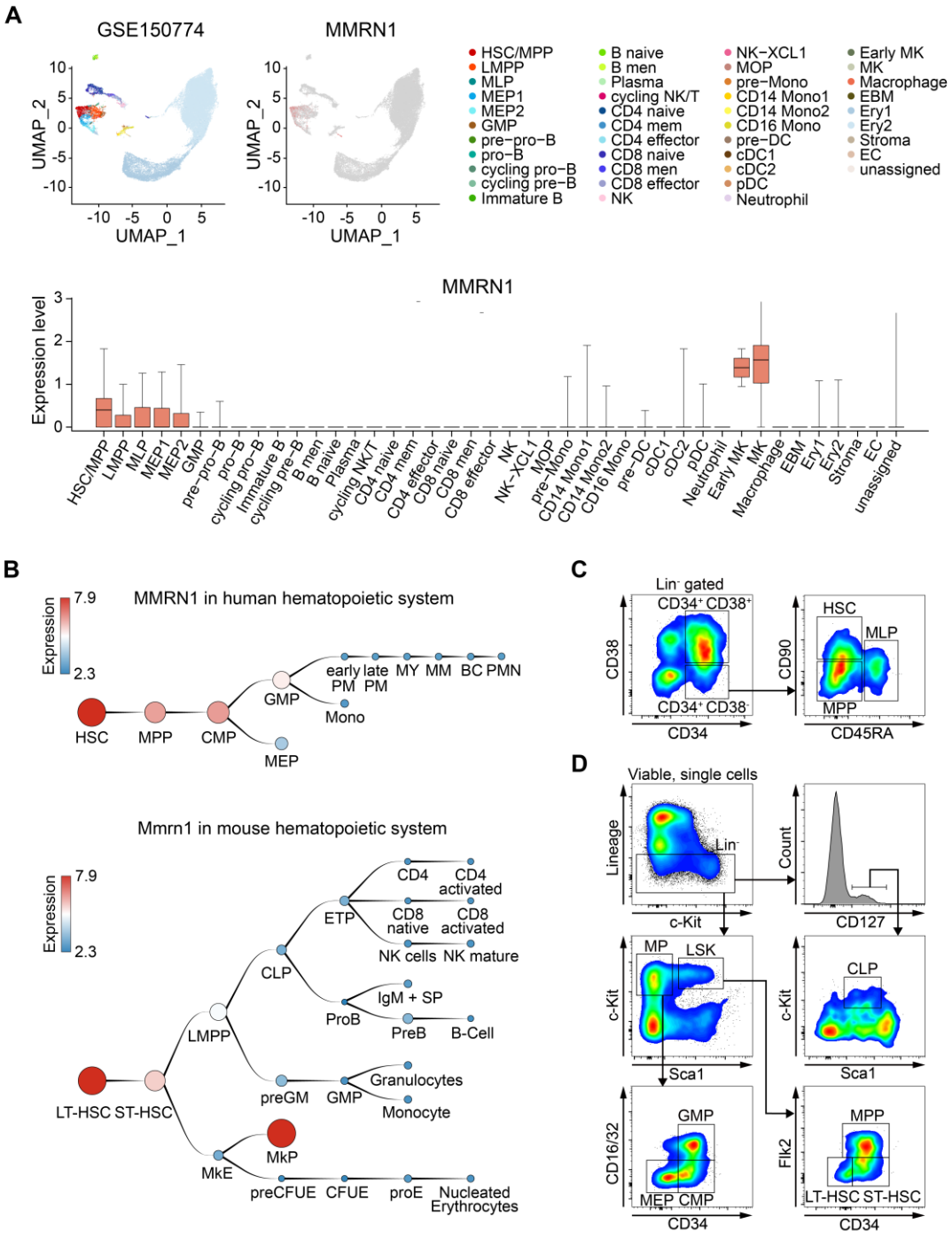

Supplementary Figure S1. The expression profile of Mmrn1 in human and murine. (A) scRNA-seq analysis of the expression of MMRN1 in human BM and UCB cells (GSE150774) from the Atlas of Blood Cells database. (B) The expression of Mmrn1 in human (up) and mouse (down) hematopoietic system from the

BloodSpot database. (C) The gating strategies for flow cytometric analysis or sorting of human HSPC populations from UCB: HSCs (Lineage$^-$ CD34$^+$ CD38$^-$ CD45RA$^-$ CD90$^+$), MPPs (Lineage$^-$ CD34$^+$ CD38$^-$ CD45RA$^-$ CD90$^-$) and MLPs (Lineage$^-$ CD34$^+$ CD38$^-$ CD45RA$^+$). (D) The gating strategies for flow cytometric analysis or sorting of mouse HSPC populations from BM: Lin$^-$ cells (Lineage$^-$), MPs (Lineage$^-$ Sca1$^-$ c-Kit$^+$), LSKs (Lineage$^-$ Sca1$^+$ c-Kit$^+$), LT-HSCs (Lineage$^-$ Sca1$^+$ c-Kit$^+$ CD34$^-$ Flk2$^-$), ST-HSCs (Lineage$^-$ Sca1$^+$ c-Kit$^+$ CD34$^+$ Flk2$^-$), MPPs (Lineage$^-$ Sca1$^+$ c-Kit$^+$ CD34$^+$ Flk2$^+$), CLPs (Lineage$^-$ CD127$^+$ Sca1^{low} c-Kit^{low}), CMPs (Lineage$^-$ Sca1$^-$ c-Kit$^+$ CD16/32$^-$ CD34$^+$), GMPs (Lineage$^-$ Sca1$^-$ c-Kit$^+$ CD16/32$^+$ CD34$^+$) and MEPs (Lineage$^-$ Sca1$^-$ c-Kit$^+$ CD16/32$^-$ CD34$^-$) .

Supplementary Figure S2

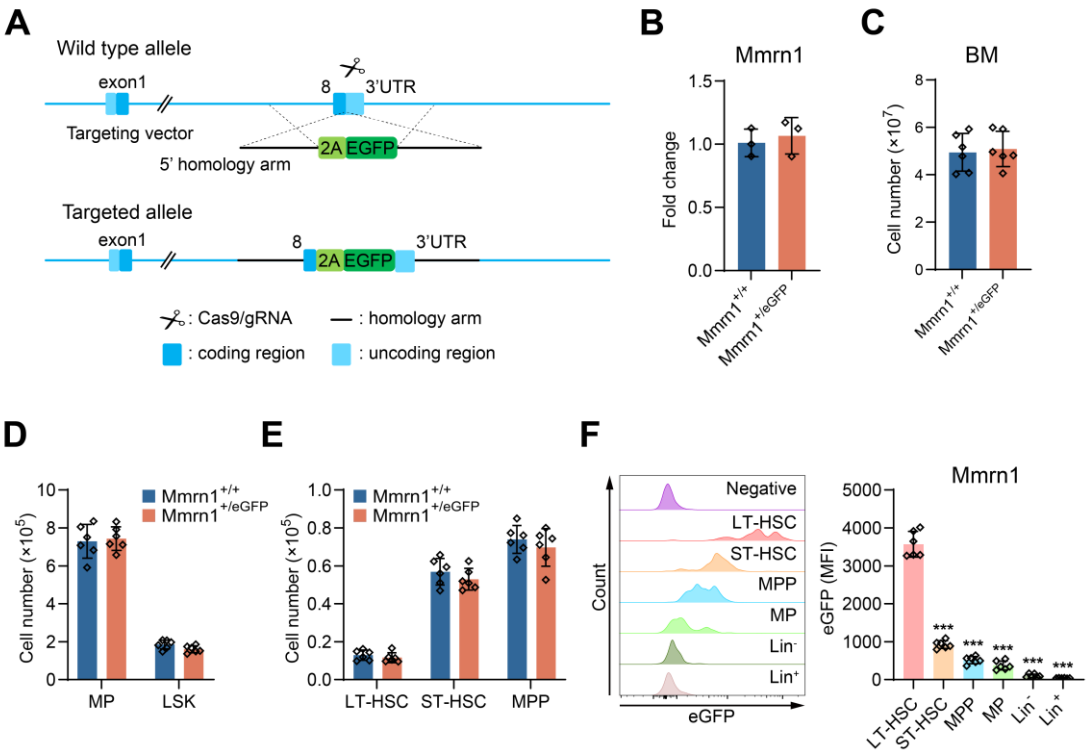

Supplementary Figure S2. The generation of Mmrn1$^{+/eGFP}$ mice. (A) The strategy for generating the Mmrn1$^{+/eGFP}$ mouse model. (B) qPCR analysis of Mmrn1 mRNA expression in LT-HSCs from the BM of Mmrn1$^{+/+}$ and Mmrn1$^{+/eGFP}$ mice (n = 3). (C-E) The numbers of (C) total BM cells and (D, E) indicated HSPC populations in two tibias and femurs from Mmrn1$^{+/+}$ and Mmrn1$^{+/eGFP}$ mice (n = 6). (F) Flow cytometric analysis of Mmrn1-eGFP expression in the indicated hematopoietic cell populations from the BM of Mmrn1$^{+/eGFP}$ mice (n = 6). WT mice served as negative controls. Representative flow cytometric plots are shown in the left. Statistical differences were analyzed by comparing each group with LT-HSCs. Data are shown as the mean ± SD. ***P < 0.001.

Supplementary Figure S3

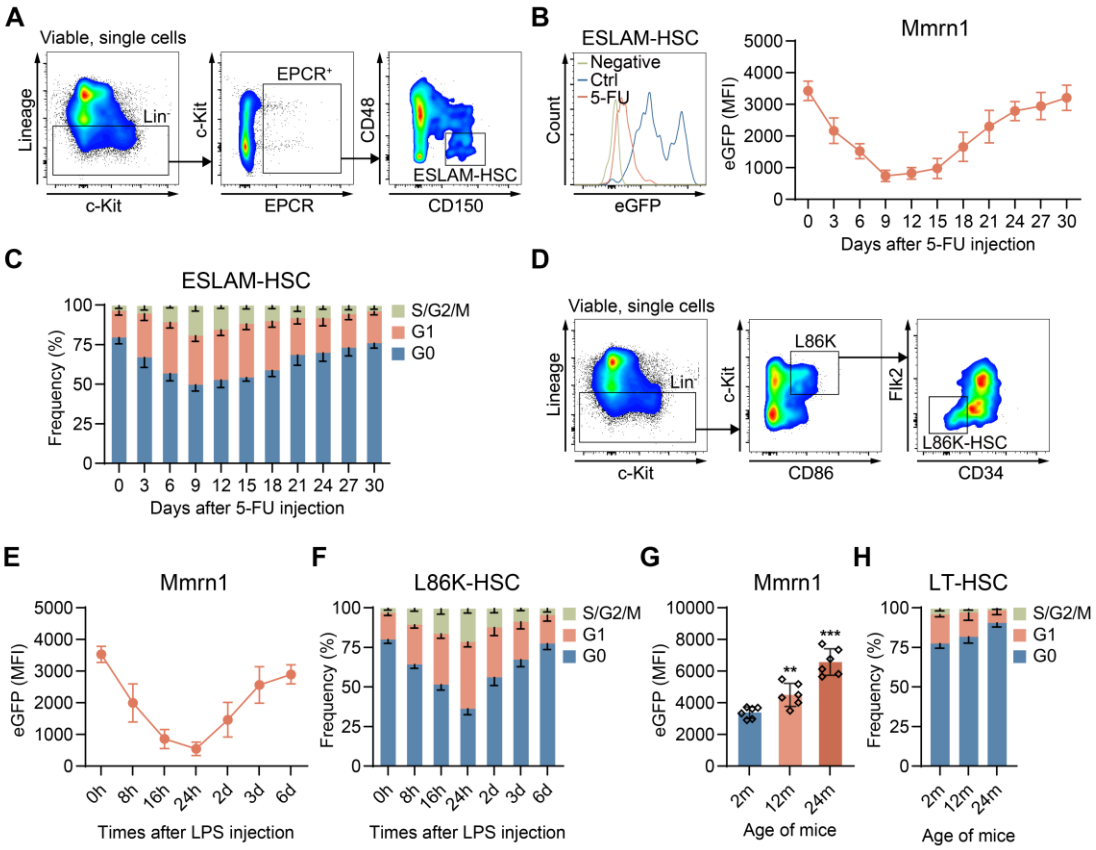

Supplementary Figure S3. Mmrn1 expression is changed in HSCs after various stresses. (A) The gating strategies for flow cytometric analysis of ESLAM-HSCs (Lineage$^-$ EPCR$^+$ CD150$^+$ CD48$^-$) after IR or 5-FU treatment. (B) Flow cytometric analysis of Mmrn1-eGFP expression in ESLAM-HSCs from the BM of Mmrn1$^{+/eGFP}$ mice at the indicated time points after 5-FU injection (n = 6 per time point). WT mice were served as negative controls. Representative flow cytometric plots at 9 days after 5-FU injection are shown in the left. (C) Cell cycle analysis of ESLAM-HSCs from the BM of Mmrn1$^{+/eGFP}$ mice at the indicated time points after 5-FU injection (n = 6 per time point). (D) The gating strategies for flow cytometric analysis of L86K-HSCs (Lineage$^-$ CD86$^+$ c-Kit$^+$ Flk2$^-$ CD34$^-$) after LPS treatment. (E, F) Flow cytometric analysis of (E) Mmrn1-eGFP expression and (F) cell cycle state in L86K-HSCs from

the BM of Mmrn1$^{+/eGFP}$ mice at the indicated time points after LPS injection (n = 6 per time point). h, hour. (G, H) Flow cytometric analysis of (G) Mmrn1-eGFP expression and (H) cell cycle state in LT-HSCs from the BM of Mmrn1$^{+/eGFP}$ mice at the indicated age (n = 6 per time point). m, month. Data are shown as the mean ± SD. **P < 0.01, ***P < 0.001.

Supplementary Figure S4

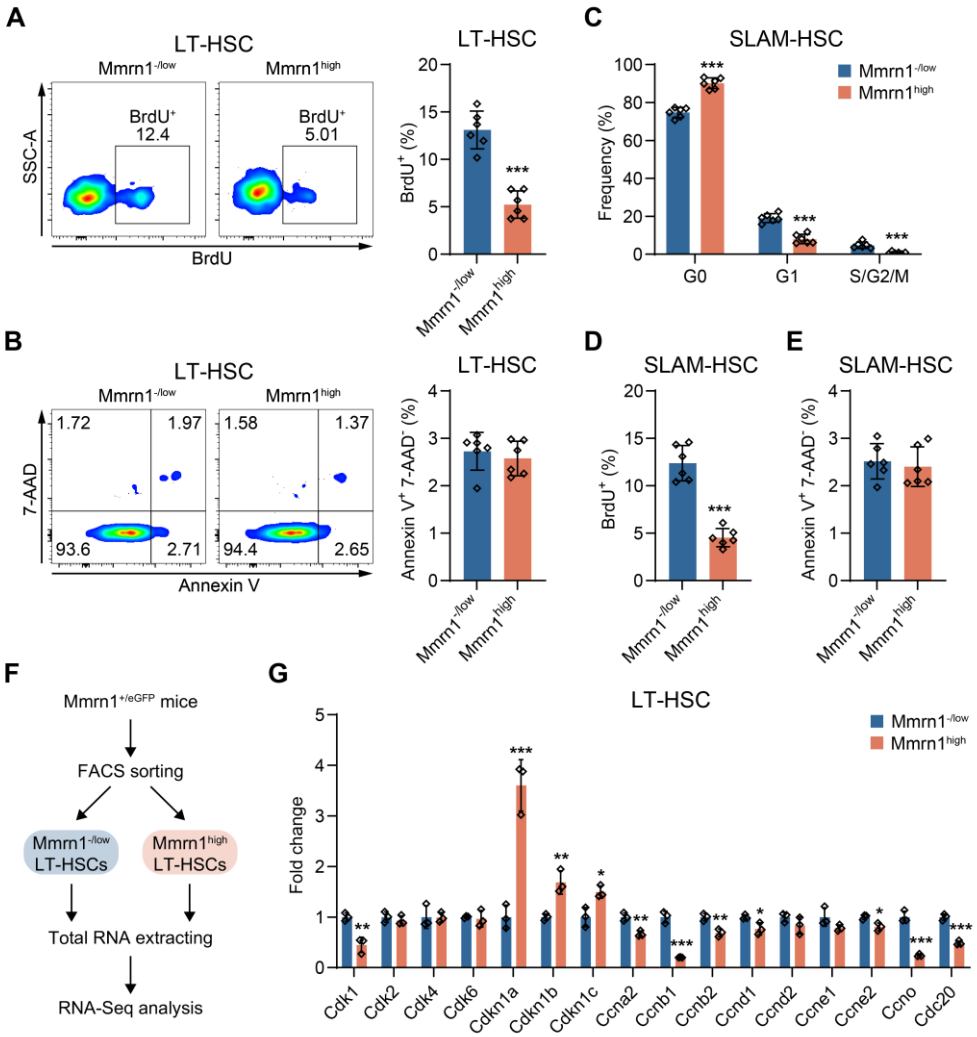

Supplementary Figure S4. Mmrn1 expression distinguishes different subgroups of HSCs. (A) The percentage of BrdU^{+} cells in Mmrn1$^{-/low}$ and Mmrn1^{high} LT-HSCs from the BM of Mmrn1$^{+/eGFP}$ mice (n = 6). (B) Apoptosis analysis of Mmrn1$^{-/low}$ and Mmrn1^{high} LT-HSCs from the BM of Mmrn1$^{+/eGFP}$ mice (n = 6). (C) Cell cycle analysis of Mmrn1$^{-/low}$ and Mmrn1^{high} SLAM-HSCs from the BM of Mmrn1$^{+/eGFP}$ mice (n = 6). (D) The percentage of BrdU^{+} cells in Mmrn1$^{-/low}$ and Mmrn1^{high} SLAM-HSCs from the BM of Mmrn1$^{+/eGFP}$ mice (n = 6). (E) Apoptosis analysis of Mmrn1$^{-/low}$ and Mmrn1^{high} SLAM-HSCs from the BM of Mmrn1$^{+/eGFP}$ mice (n = 6). (F) Schematic diagram of the RNA-seq analysis (n = 3). (G) qPCR analysis of mRNA

expression of the indicated genes in Mmrn1$^{-/low}$ and Mmrn1^{high} LT-HSCs sorted from the BM of Mmrn1$^{+/eGFP}$ mice (n = 3). Data are shown as the mean ± SD. *P < 0.05, **P < 0.01, ***P < 0.001.

Supplementary Figure S5

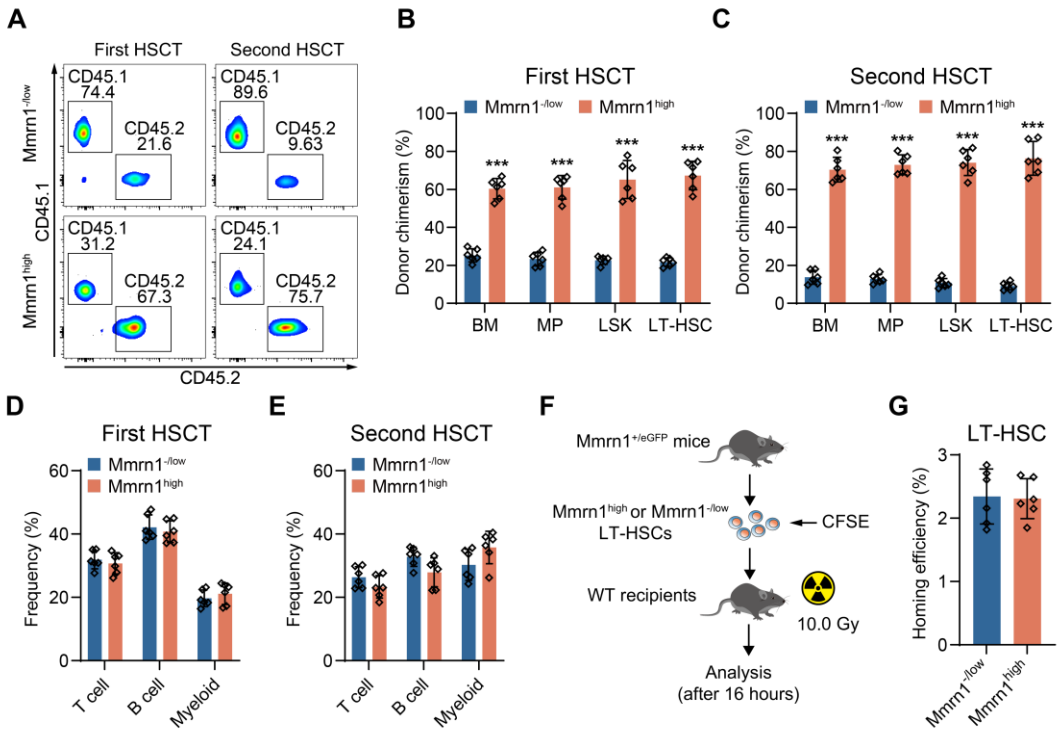

Supplementary Figure S5. Mmrn1$^{-/low}$ and Mmrn1^{high} HSCs show different abilities in long-term reconstitution but not in homing and differentation. (A) Representative flow cytometric plots showing the chimerism levels of LT-HSCs in the BM of recipients at 16 weeks after the first and second HSCT. (B, C) The chimerism levels of donor-derived BM cells, MPs, LSKs and LT-HSCs in the recipients at 16 weeks after the (B) first and (C) second HSCT (n = 6). (D, E) The lineage distribution of donor-derived cells in the PB of recipients at 16 weeks after the (D) first and (E) second HSCT (n = 6). (F) The schematic diagram of homing assay. (G) The homing efficiency of Mmrn1$^{-/low}$ and Mmrn1^{high} LT-HSCs from the BM of Mmrn1$^{+/eGFP}$ mice (n = 6). Data are shown as the mean ± SD. ***P < 0.001.

Supplementary Figure S6

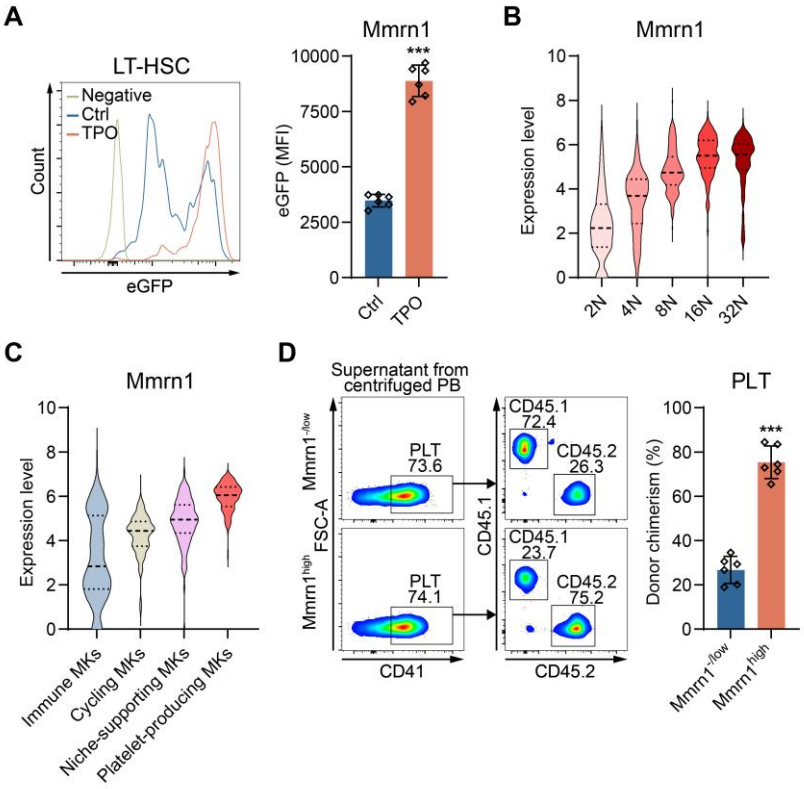

Supplementary Figure S6. Mmrn1 marks megakaryocytic lineage commitment. (A) Flow cytometric analysis of Mmrn1-eGFP expression in LT-HSCs from the BM of Mmrn1$^{+/eGFP}$ mice at 48 hours after 50 μg/kg TPO injection (n = 6). WT mice were served as negative controls. Representative flow cytometric plots are shown in the left. (B, C) Mmrn1 expression in (B) the ploidy clusters and (C) the subpopulations of mouse megakaryocytes from the OMIX database under reference number OMIX005321. Mk, megakaryocyte. (D) The chimerism levels of PLT in the PB of recipient mice were determined at 2 weeks after transplanted with Mmrn1$^{-/low}$ and Mmrn1^{high} LT-HSCs (n = 6). Representative flow cytometric plots are shown in the left. Data are shown as the mean ± SD. ***P < 0.001.

Supplementary Figure S7

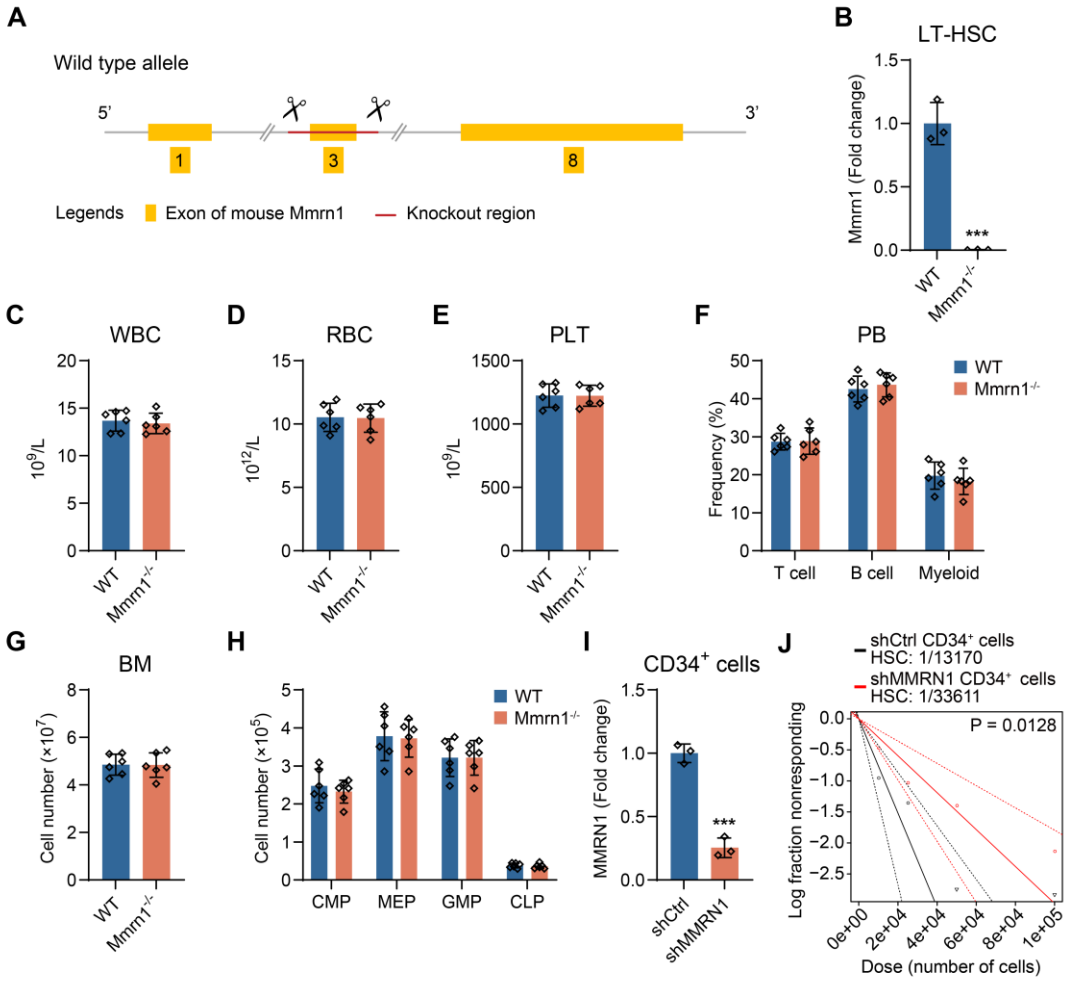

Supplementary Figure S7. Mmrn1 deficiency does not significantly affect normal hematopoietic parameters. (A) The strategy of generation of the Mmrn1$^{-/-}$ mouse model. (B) qPCR analysis of Mmrn1 mRNA expression in LT-HSCs from the BM of WT and Mmrn1$^{-/-}$ mice (n = 3). (C-E) The counts of (C) WBC, (D) RBC and (E) PLT in the PB of WT and Mmrn1$^{-/-}$ mice (n = 6). (F) The percentages of T cells, B cells and myeloid cells in PB of WT and Mmrn1$^{-/-}$ mice (n = 6). (G) The number of total BM cells in two tibias and femurs from WT and Mmrn1$^{-/-}$ mice (n = 6). (H) The numbers of CMPs, MEPs, GMPs and CLPs in two tibias and femurs from WT and Mmrn1$^{-/-}$ mice (n = 6). (I) qPCR analysis of MMRN1 mRNA expression in human

UCB $CD34^+$ cells after transfected with shCtrl or shMMRN1 (n = 3). (J) Limiting dilution analysis of the functional HSC frequency in human UCB $CD34^+$ cells after transfected with shCtrl or shMMRN1 (n = 8). Data are shown as the mean ± SD. ***P < 0.001.

Supplementary Figure S8

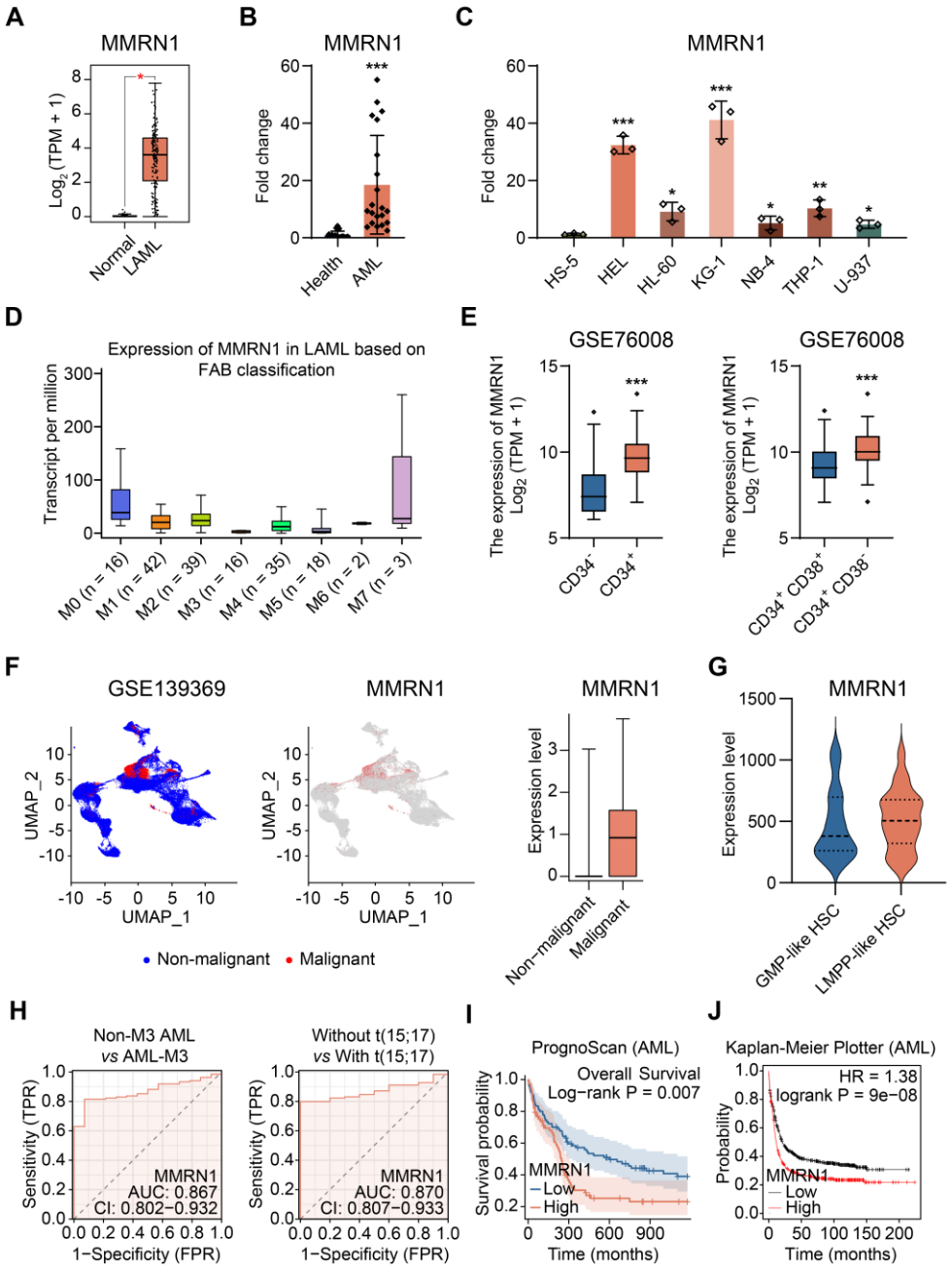

Supplementary Figure S8. High expression of MMRN1 portends a poor prognosis in patients with AML. (A) The expression of MMRN1 in 173 AML patients and 70 healthy donors from the GEPIA2 database. (B) qPCR analysis of MMRN1 expression in the BM samples obtained from 21 AML patients and 17 healthy donors. (C) qPCR analysis of MMRN1 mRNA expression in HS-5, HEL, HL-

60, KG-1, NB-4, THP-1 and U-937 cells (n = 3). Statistical differences were analyzed by comparing each group with HS-5 cells. (D) The expression of MMRN1 in LAML samples based on FAB classification from the UALCAN database. (E) The expression of MMRN1 in (left) $CD34^-/CD34^+$ and (right) $CD34^+$ $CD38^+/CD34^+$ $CD38^-$ AML samples (GSE76008). (F) scRNA-seq analysis of the expression of MMRN1 in AML samples (GSE139369) from the Atlas of Blood Cells database. (G) The expression of MMRN1 in GMP-like LSCs and LMPP-like LSCs (E-TABM-978). (H) ROC analysis of the diagnostic performance of MMRN1 for the indicated binary classification from the UCSC XENA database. (I, J) Survival curves of AML patients with low or high expression of MMRN1. Data were obtained from the (I) PrognoScan database and (J) Kaplan-Meier plotter database. Data are shown as the mean ± SD. *P < 0.05, **P < 0.01, ***P < 0.001.

Supplementary Figure S9

A

Transcription Factor Binding at the MMRN1 locus

Cell Type	HSC	CMP	GMP	MEP	KG1	ME1	KAS1	TSU
ERG	×	✓	×	×	×	✓	✓	✓
FLI1	✓	✓	✓	✓	✓	×	✓	✓
GATA2	✓	✓	✓	✓	✓	×	×	✓
RUNX1	✓	✓	✓	✓	✓	✓	✓	✓
TAL1	✓	✓	×	✓	×	×	✓	✓
LYL1	✓	✓	✓	✓	✓	×	✓	✓
LMO2	✓	✓	✓	✓	×	×	×	✓
PU.1	×	✓	✓	✓	✓	×	✓	✓
STAG2	✓	✓	×	✓	▢	▢	▢	▢
CTCF	✓	✓	✓	✓	▢	▢	▢	▢

B

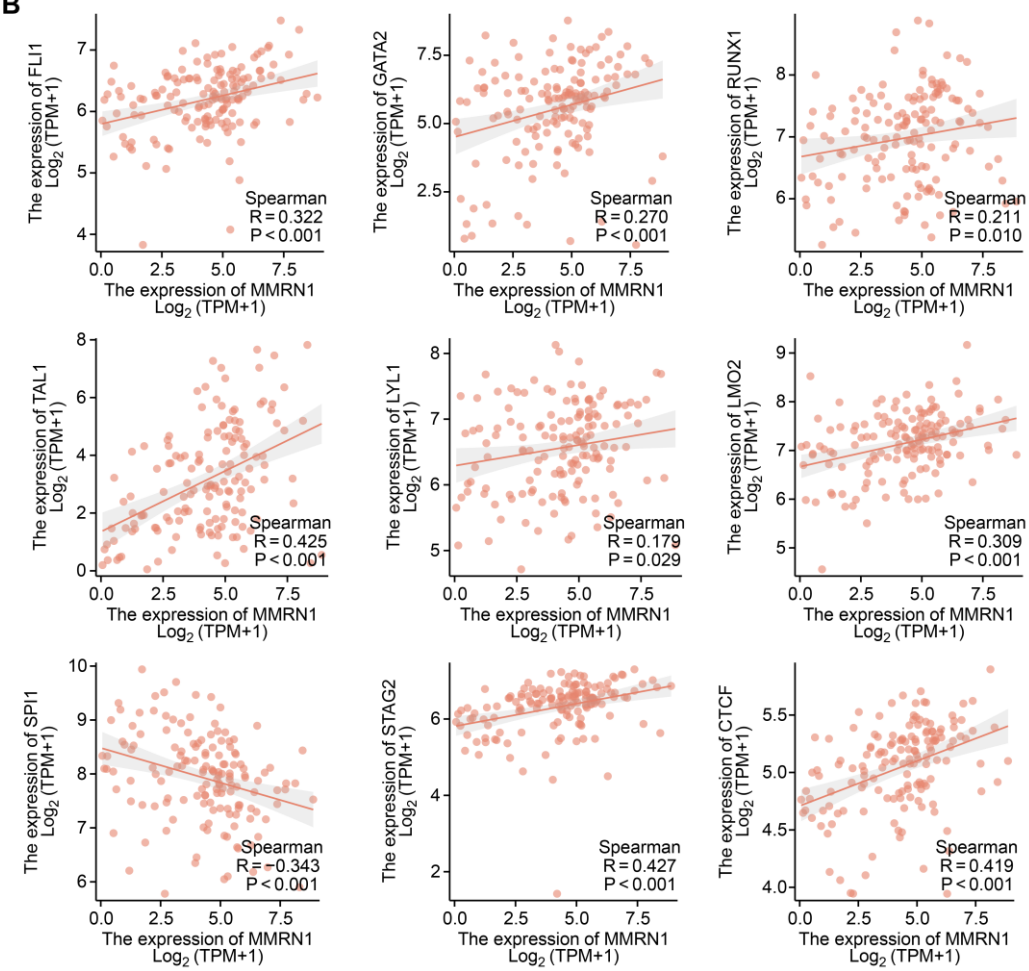

Supplementary Figure S9. The correlation of MMRN1 with several hematopoiesis-related transcription factors. (A) Analysis of transcription factor

binding at the MMRN1 locus in the indicated types of cells from the BloodChIP Xtra database. (B) The correlation analysis of the expression of MMRN1 and the indicated transcription factors in AML samples from the TCGA database. The transcription factor PU.1 is encoded by SPI1.

Supplementary Figure S10

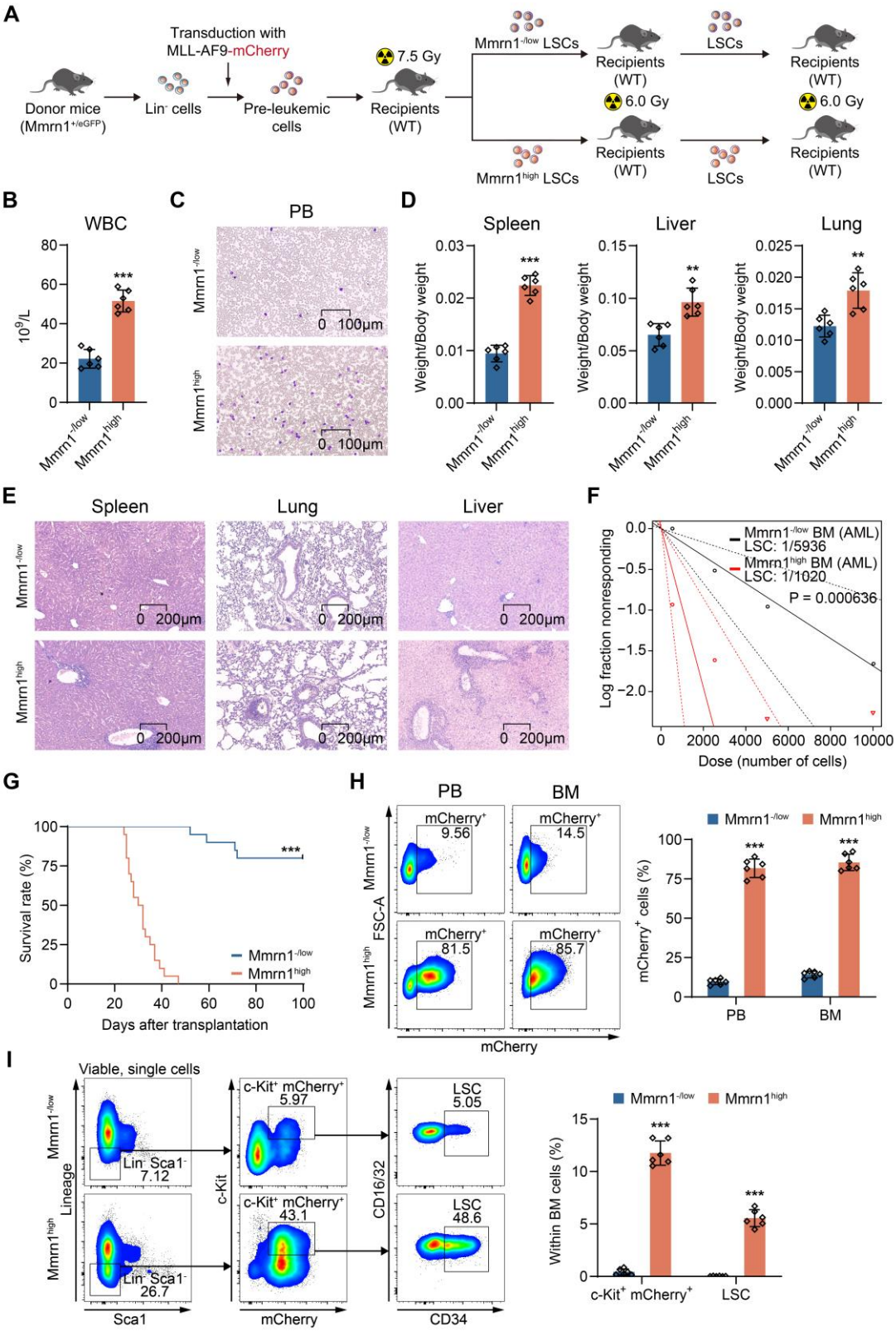

Supplementary Figure S10. Mmrn1^{high} LSCs are responsible for AML development. (A) Schematic diagram of generating MLL-AF9-induced leukemia mouse model. (B) The count of WBC in the PB of recipients at 25 days after transplanted with Mmrn1$^{-/low}$ and Mmrn1^{high} LSCs (n = 6). (C) Wright-Giemsa staining of PB smears from the second recipients at 25 days after transplanted with Mmrn1$^{-/low}$ and Mmrn1^{high} LSCs. (D) The spleen, liver and lung index (weights/body weights) of recipient mice at 25 days after transplanted with Mmrn1$^{-/low}$ and Mmrn1^{high} LSCs (n = 6). (E) Hematoxylin & eosin (H&E) staining of spleen, lung and liver of recipients at 25 days after transplanted with Mmrn1$^{-/low}$ and Mmrn1^{high} LSCs. (F) Limiting dilution analysis of the functional LSC frequency in the second recipients at 25 days after transplanted with Mmrn1$^{-/low}$ and Mmrn1^{high} LSCs (n = 5). (G) Kaplan-Meier curves of the third recipients after transplanted with Mmrn1$^{-/low}$ and Mmrn1^{high} LSCs (n = 20). (H) The percentages of mCherry^{+} cells in the PB and BM from the third recipients at 25 days after transplanted with Mmrn1$^{-/low}$ and Mmrn1^{high} LSCs (n = 6). Representative flow cytometric plots are shown in the left. (I) The percentages of c-Kit^{+} mCherry^{+} cells and LSCs in the BM of third recipients at 25 days after transplanted with Mmrn1$^{-/low}$ and Mmrn1^{high} LSCs (n = 6). Representative flow cytometric plots are shown in the left. **P < 0.01, ***P < 0.001

Supplementary Figure S11

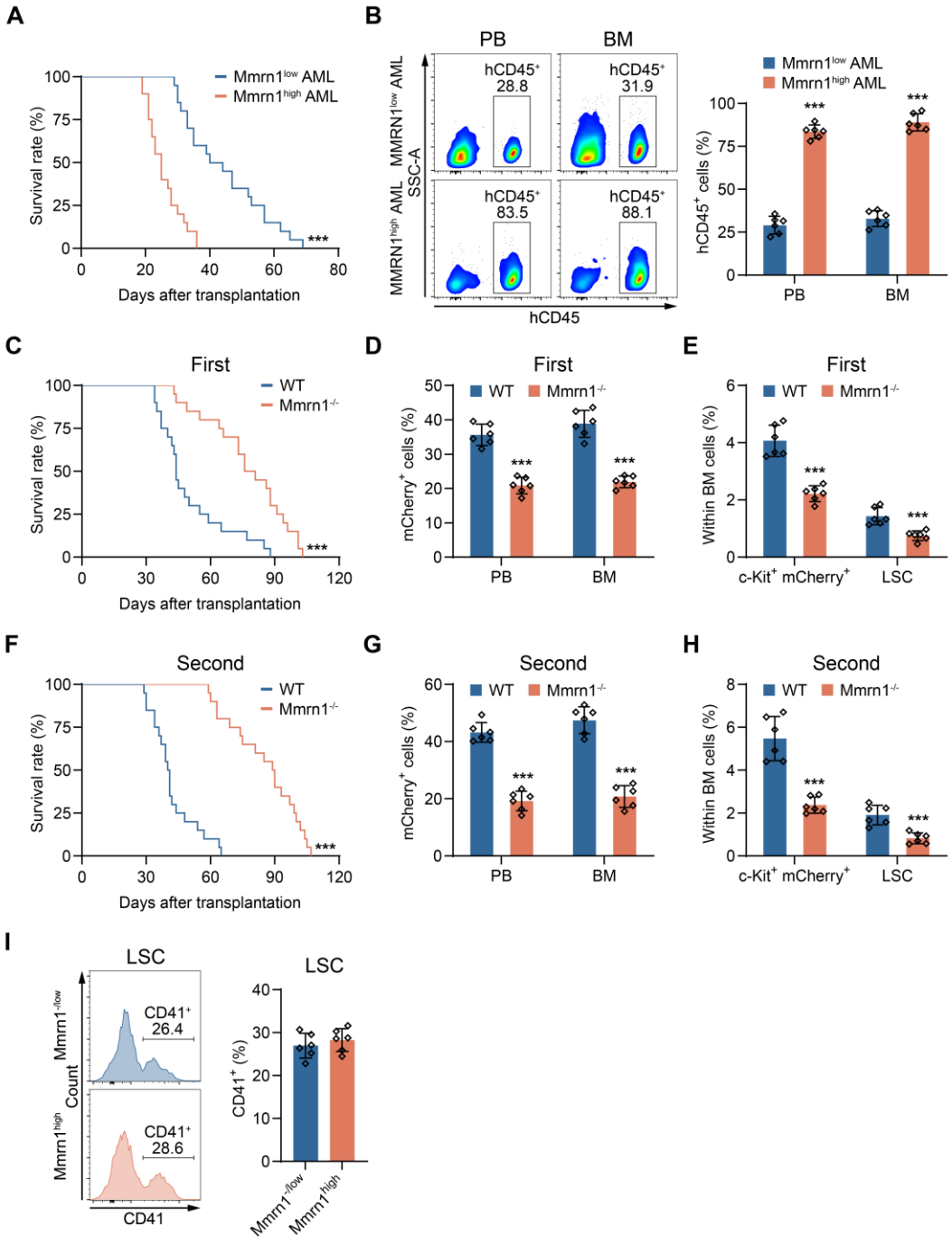

Supplementary Figure S11. Mmrn1 deficiency delays AML development. (A, B) $CD34^+$ cells isolated from human AML cases with high or low expression of MMRN1 were transplanted into sublethally irradiated (2.5 Gy) M-NSG mice. (A) Kaplan-Meier curves of the recipients after transplanted with $MMRN1^{low}$ and

MMRN1^{high} CD34^{+} AML cells (n = 20). (B) The percentage of hCD45^{+} cells in the PB and BM of recipients at 25 days after transplantation. (C-H) Lin^{-} cells isolated from WT and Mmrn1$^{-/-}$ mice were transduced with MLL-AF9 retrovirus to generate pre-leukemic cells, which were then transplanted into 7.5 Gy irradiated WT mice. Twenty-five days after transplantation, LSCs were purified from the first recipients and were transplanted into 6.0 Gy irradiated second recipients. (C, F) Kaplan-Meier curves of the (C) first and (F) second recipients after transplanted with WT and Mmrn1$^{-/-}$ LSCs (n = 20). (D, G) The percentage of mCherry^{+} cells in the PB and BM of the (D) first and (G) second recipients at 25 days after transplantation. (E, H) The percentages of c-Kit^{+} mCherry^{+} cells and LSCs in the BM of the (E) first and (H) second recipients at 25 days after transplanted with WT and Mmrn1$^{-/-}$ LSCs (n = 6). (I) The expression of CD41 in Mmrn1$^{-/low}$ and Mmrn1^{high} LSCs after TPO stimulation *in vitro* (n = 6). Data are shown as the mean ± SD. ***P < 0.001.

Supplementary Table S1

Antibodies used for flow cytometry (FC)

Antibodies for mouse	**Cat. No**	**Origin**
Alexa Fluor 700 anti-mouse CD34	56-0341-82	eBioscience
APC anti-mouse CD201 (EPCR)	141505	BioLegend
APC anti-mouse CD86	105113	BioLegend
APC anti-mouse Sca1	108112	BioLegend
APC-eFluor 780 anti-mouse CD3e	47-0031-82	eBioscience
APC-eFluor 780 anti-mouse c-Kit	47-1171-82	eBioscience
Biotin anti-mouse Lineage Panel	133307	BioLegend
Brilliant Violet 510 Annexin V	640937	BioLegend
Brilliant Violet 510 anti-mouse TER-119	116237	BioLegend
Brilliant Violet 510 Streptavidin	405234	BioLegend
eFluor 450 anti-mouse BrdU Staining Kit	8848-6600-42	Thermo Fisher
eFluor 450 anti-mouse CD16/32	48-0161-82	eBioscience
eFluor 450 anti-mouse CD45.1	48-0453-82	eBioscience
eFluor 450 anti-mouse Lineage Cocktail	88-7770-72	eBioscience
eFluor 660 anti-mouse CD34	50-0341-82	eBioscience
PE anti-mouse B220	12-0452-82	eBioscience
PE anti-mouse CD127	12-1271-82	eBioscience
PE anti-mouse CD135	12-1351-82	eBioscience
PE anti-mouse CD150	115904	BioLegend
PE anti-mouse Ki67	151210	BioLegend
PE/Cyanine5 anti-mouse CD16/32	156618	BioLegend
PE/Cyanine7 anti-mouse CD48	103424	BioLegend
PE-Cyanine7 anti-mouse Ki67	25-5698-82	eBioscience
PE-Cyanine7 anti-mouse CD45.2	25-0454-82	eBioscience
PE-Cyanine7 anti-mouse c-Kit	25-1171-82	eBioscience
PerCP-Cyanine5.5 anti-mouse CD11b	45-0112-82	eBioscience
PerCP-Cyanine5.5 anti-mouse Sca1	45-5981-82	eBioscience
Antibodies for human	**Cat. No**	**Origin**
APC anti-human CD38	303510	BioLegend
Brilliant Violet 510 anti-human Lineage Cocktail	348807	BioLegend
PE anti-human CD34	343506	BioLegend
PE-Cyanine5 anti-human CD90	328112	BioLegend
PE-Cyanine7 anti-human CD45RA	304126	BioLegend
APC anti-human CD45	304012	BioLegend

Supplementary Table S2

Primers for mRNA expression analysis

Gene in mouse	**Forward primer (5'-3')**	**Reverse primer (5'-3')**
Cdkn1a	CCTGGTGATGTCCGACCTG	CCATGAGCGCATCGCAATC
Cdkn1b	TCAAACGTGAGAGTGTCTAACG	CCGGGCCGAAGAGATTTCTG
Cdkn1c	CGAGGAGCAGGACGAGAATC	GAAGAAGTCGTTCGCATTGGC
Ccnb1	AAGGTGCCTGTGTGTGAACC	GTCAGCCCCATCATCTGCG
Ccnb2	GCCAAGAGCCATGTGACTATC	CAGAGCTGGTACTTTGGTGTTC
Ccnd1	GCACAACGCACTTTCTTTCCA	GATGGAGGGGGTCCTTGTTTAG
Ccnd2	CATTCAGACACAGGACTT	GTATAGATGCCAAGAAGGAA
Ccne1	CCGTCTTGAATTGGGGCAATA	GAGCTTATAGACTTCGCACACC
Ccne2	TCAGCCCTTGCATTATCATTGAA	CCAGCTTAAATCTGGCAGAGG
Cdk1	AGAAGGTACTTACGGTGTGGT	GAGAGATTTCCCGAATTGCAGT
Cdk2	ACTGAGACTGAAGGTGTA	TTGACGATATTAGGGTGATTA
Ckd4	TGATGGATGTCTGTGCTA	TCCTGGTCTATATGCTCAA
Ckd6	TGGACATCATTGGACTCCCAG	TCGATGGGTTGAGCAGATTTG
Ccno	GTCTGTGACCTTTTCGAGTCC	CTCTGGCCGTATTCTCGGA
Cdc20	TTCGTGTTCGAGAGCGATTTG	ACCTTGGAACTAGATTTGCCAG
Gata1	TGGGGACCTCAGAACCCTTG	GGCTGCATTTGGGGAAGTG
Gata2	CGACGAGGTGGATGTCTTCT	ACAAGTGTGGTCGGCACAT
Fli1	ATGGACGGGACTATTAAGGAGG	GAAGCAGTCATATCTGCCTTGG
Runx1	GATGGCACTCTGGTCACCG	GCCGCTCGGAAAAGGACAA
Mpl	AACCCGGTATGTGTGCCAG	AGTTCATGCCTCAGGAAGTCA
Gp9	TGCGACCACAGATACTCAGG	ACTGAACGCAGGCTATTGTTG
Zfpm1	CCTTGCTACCGCAGTCATCA	ACCAGATCCCGCAGTCTTTG
Tal1	CGCTGCTCTATAGCCTTAGCC	CTCTTCACCCGGTTGTTGTT
Mmrn1	ACCACCATTCTGATAGGCCG	GATCTCCCGCTGATGCATGT
Gapdh	CCTCGTCCCGTAGACAAAATG	TCTCCACTTTGCCACTGCAA
Gene in human	**Forward primer (5'-3')**	**Reverse primer (5'-3')**
MMRN1	TACAGAGAGGCCAAGAGGTT	TCGGTTTCCTGTTTCTGTAGGG
GAPDH	GGAGTCCACTGGCGTCTTCA	GTCATGAGTCCTTCCACGATACC

Supplementary Table S3

Baseline patient characters with respect to MMRN1 expression

Clinical characters	$MMRN1^{low}$ (n=75)	$MMRN1^{high}$ (n=75)	*p* value
Gender, n (%)			0.622
Female	35 (23.3%)	32 (21.3%)	
Male	40 (26.7%)	43 (28.7%)	
Age, n (%)			0.620
<= 60	45 (30%)	42 (28%)	
> 60	30 (20%)	33 (22%)	
WBC count (×10^9/L), n (%)			0.933
<= 20	38 (25.5%)	38 (25.5%)	
> 20	36 (24.2%)	37 (24.8%)	
BM blasts (%), n (%)			0.012
<= 20	37 (24.7%)	22 (14.7%)	
> 20	38 (25.3%)	53 (35.3%)	
PB blasts (%), n (%)			0.252
<= 70	32 (21.3%)	39 (26%)	
> 70	43 (28.7%)	36 (24%)	
Cytogenetic risk, n (%)			< 0.001
Favorable	23 (15.5%)	7 (4.7%)	
Intermediate/normal	44 (29.7%)	38 (25.7%)	
Poor	7 (4.7%)	29 (19.6%)	
FAB classifications, n (%)			< 0.001
M0	3 (2.9%)	12 (11.8%)	
M1	14 (13.7%)	21 (20.6%)	
M2	13 (12.7%)	25 (24.5%)	
M3	14 (9.4%)	0 (0%)	
M4	19 (12.8%)	10 (6.7%)	
M5	11 (7.4%)	4 (2.7%)	
M6	1 (0.7%)	1 (0.7%)	
M7	0 (0%)	1 (0.7%)	
Cytogenetics, n (%)			< 0.001
Normal	38 (32.2%)	31 (26.3%)	
inv(16)	2 (1.7%)	6 (5.1%)	
t(15;17)	10 (8.5%)	0 (0%)	
t(8;21)	6 (5.1%)	1 (0.8%)	
Complex	6 (5.1%)	18 (15.3%)	
FLT3 mutation, n (%)			0.751
Negative	51 (34.9%)	50 (34.2%)	
Positive	24 (16.4%)	21 (14.4%)	
NPM1 mutation, n (%)			0.012
Negative	52 (34.9%)	64 (43%)	
Positive	23 (15.4%)	10 (6.7%)	
RAS mutation, n (%)			0.702
Negative	72 (48.3%)	69 (46.3%)	
Positive	3 (2%)	5 (3.4%)	

n, number of patients; FAB, French-American-British